The Abdus Salam
International Centre for Theoretical Physics

United Nations
Educational, Scientific and
Cultural Organization

IAEA
International Atomic Energy Agency

2141-19

Joint ICTP-IAEA Workshop on Nuclear Reaction Data for Advanced Reactor Technologies

3 - 14 May 2010

The Optical Model and Direct Reactions

CARLSON B.V.
ITA-CTA, Sao Jose dos Campos
Sao Paulo
BRAZIL

The Optical Model

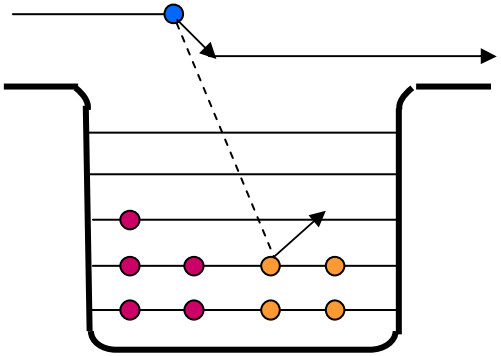

and Direct Reactions

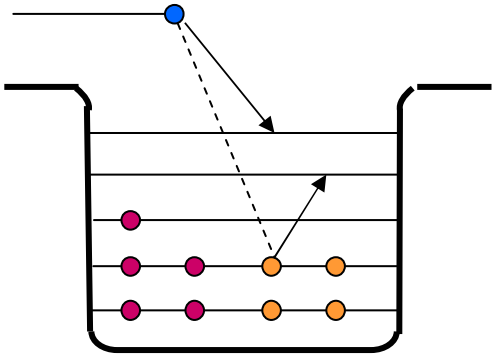

B.V. Carlson -- Depto. de Física
Instituto Tecnológico de Aeronáutica
São José dos Campos SP, Brazil

The quantum view of scattering

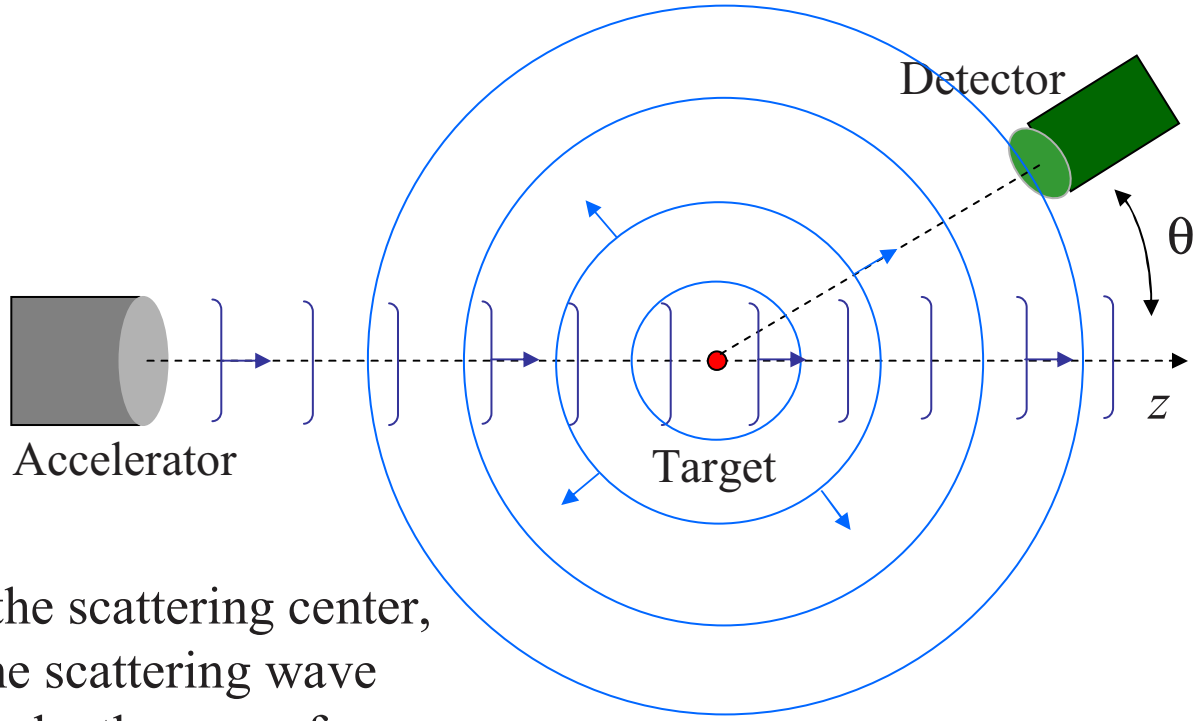

Far from the scattering center, we take the scattering wave function to be the sum of a plane wave and a scattered outgoing spherical wave,

$$\psi(\vec{r}) \approx e^{ikz} + f(\theta)\frac{e^{ikr}}{r}.$$

when $r \to \infty$. $\left(k^2 = 2\mu E_{cm}/\hbar^2\right)$

The differential cross section is the squared magnitude of the scattering amplitude,

$$\frac{d\sigma}{d\Omega} = |f(\theta)|^2 .$$

Back to the basics

We defined the differential cross section as

$$d\sigma = \frac{\text{particle intensity entering detector of solid angle } d\Omega}{\text{(incident intensity/area) * (no. of target particles in beam)}} = \frac{n(\theta)\,d\Omega}{(n_0/A)(\rho_{tar}tA)}$$

How did we relate this with the asymptotic form of the wave function

$$\psi(\vec{r}) \approx e^{ikz} + f(\theta)\frac{e^{ikr}}{r}. \qquad \text{to obtain} \qquad \frac{d\sigma}{d\Omega} = |f(\theta)|^2 \ ?$$

- First, we assume that we have but one target nucleus, $\rho_{tar}tA = 1$.
- Next, we note that n_0/A is proportional to the plane wave current density,

$$n_0/A = \frac{\hbar}{2i\mu}\left(\psi_{in}^*\nabla\psi_{in} - (\nabla\psi_{in}^*)\psi_{in}\right) = \frac{\hbar k}{\mu} = v \quad \text{since} \quad \psi_{in} = e^{ikz}.$$

- Finally, we write the particle intensity entering the detector in terms of the current density of scattered particles,

$$n(r,\theta)d\Omega = \frac{\hbar}{2i\mu}\left(\psi_{sc}^*\partial_r\psi_{sc} - (\partial_r\psi_{sc}^*)\psi_{sc}\right)(r^2 d\Omega) \xrightarrow[r\to\infty]{} v|f(\theta)|^2.$$

The partial-wave expansion

Neglecting spin for the moment, we use conservation of angular momentum to expand the wave function in partial waves of the orbital angular momentum,

$$\psi(r,\theta) = \sum_{l=0}^{\infty} u_l(r) P_l(\cos\theta).$$

The plane wave may be expanded as

$$e^{ikz} = \sum_{l=0}^{\infty} (2l+1) i^l j_l(kr) P_l(\cos\theta)$$

with

$$j_l(kr) = \frac{i}{2}\left(h_l^{(-)}(kr) - h_l^{(+)}(kr)\right) \qquad \text{where} \qquad h_l^{(\pm)}(kr) \xrightarrow[r\to\infty]{} (\mp i)^l \frac{e^{\pm ikr}}{kr}.$$

In analogy with the plane wave, we write

$$\psi(r,\theta) = \sum_{l=0}^{\infty} (2l+1) i^l \psi_l(r) P_l(\cos\theta)$$

where each of the partial waves satisfies the Schrödinger equation

$$\left(\frac{\partial^2}{\partial r^2} + k^2 - \frac{2\mu}{\hbar^2}U(r) - \frac{l(l+1)}{r^2}\right)\left(r\psi_l(r)\right) = 0.$$

More on the partial-wave expansion

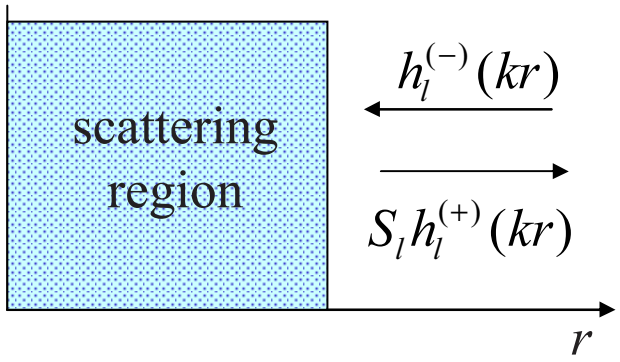

Outside the scattering region defined by the potential $U(r)$, the wave function $\psi_l(r)$ satisfies the same Schrödinger equation as the plane wave and must be a linear combination of the same incoming / outgoing waves $h_l^{(\pm)}(kr)$,

$$\psi_l(r) \to \frac{i}{2}\left(h_l^{(-)}(kr) - S_l h_l^{(+)}(kr)\right).$$

The incoming wave must be the same as that of the plane wave, so that the only difference with the plane wave is in the outgoing scattered wave.

Substituting in the partial wave expansion,

$$\psi(r,\theta) \to \sum_{l=0}^{\infty}(2l+1)i^l\left(j_l(kr) + \frac{S_l - 1}{2i}h_l^{(+)}(kr)\right)P_l(\cos\theta)$$

$$\to e^{ikz} + \frac{1}{2ik}\sum_{l=0}^{\infty}(2l+1)\left(S_l - 1\right)P_l(\cos\theta)\frac{e^{ikr}}{r},$$

so that

$$f(\theta) = \frac{1}{2ik}\sum_{l=0}^{\infty}(2l+1)\left(S_l - 1\right)P_l(\cos\theta) = \frac{4\pi}{2ik}\sum_{lm}\left(S_l - 1\right)Y_{lm}(\hat{r})Y_{lm}^*(\hat{k}).$$

Solving the scattering problem

How do we obtain the asymptotic form of the wave function,

$$\psi_l(r) \to \frac{i}{2}\left(h_l^{(-)}(kr) - S_l h_l^{(+)}(kr)\right)?$$

First, we fix a radius r_m, called the matching radius, that is beyond the range of the interaction.

The wave function inside the matching radius, ψ_{in}, is determined numerically, up to a multiplicative factor. Outside the matching radius, the wave function has the asymptotic form,

$$\psi_{l,ex}(r) = \frac{i}{2}\left(h_l^{(-)}(kr) - S_l h_l^{(+)}(kr)\right).$$

We require continuity of the wave function and its derivative at the matching radius.

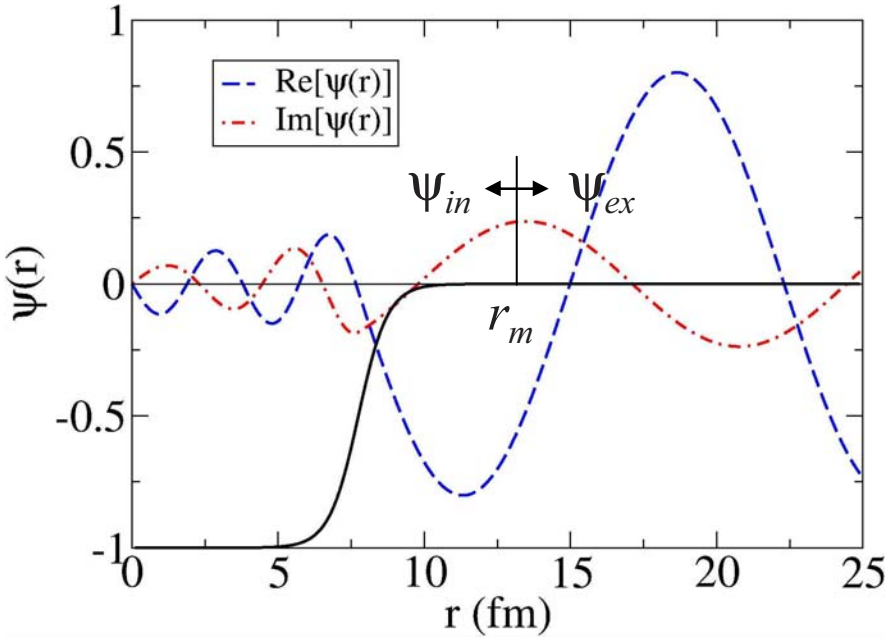

This gives us two equation in two unknowns, A_l and S_l,

$$A_l \psi_{l,in}(r_m) = \frac{i}{2}\left(h_l^{(-)}(kr_m) - S_l h_l^{(+)}(kr_m)\right)$$

and the derivative equation. We solve these for each value of l, stopping when S_l is sufficiently close to one.

Integrated cross sections

We obtain the elastic cross section by integrating over the differential one,

$$\sigma_{el} = 2\pi \int_0^{\pi} |f(\theta)|^2 \sin\theta d\theta = \frac{\pi}{k^2} \sum_{l=0}^{\infty} (2l+1) |S_l - 1|^2 .$$

We may calculate the absorption cross section by taking into account all of the flux entering and leaving the scattering region. Integrating the flux over a sphere whose radius tends to infinity, we have

$$\sigma_{abs} = -\frac{1}{v} \int_S \vec{j} \cdot d\vec{S} = \frac{\pi}{k^2} \sum_{l=0}^{\infty} (2l+1) \left(1 - |S_l|^2\right).$$

The total cross section takes into account all flux lost from the incident plane wave, either by scattering or absorption,

$$\sigma_{tot} = \sigma_{el} + \sigma_{abs} = \frac{2\pi}{k^2} \sum_{l=0}^{\infty} (2l+1) \left(1 - \mathrm{Re}\, S_l\right).$$

The total cross section satisfies the optical theorem,

$$\sigma_{tot} = \frac{4\pi}{k} \mathrm{Im}\, f(\theta = 0^\circ).$$

Direct and compound nuclear scattering

At low energies, neutron-nucleus scattering occurs either directly or through the qausi-bound compound nucleus states.

Direct scattering

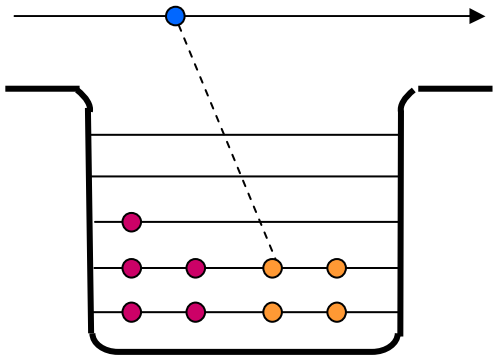

$\Delta t \sim 10^{-20} - 10^{-22}$ s

$\Delta E \Delta t \geq \hbar$

Compound nuclear scattering

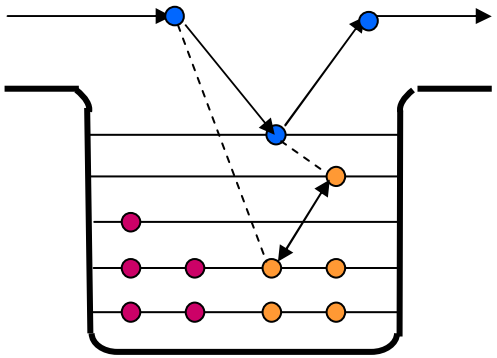

$\Delta t \sim 10^{-12} - 10^{-20}$ s

In a direct scattering, the incident neutron interacts with the average field of the nucleus. The duration of the collision is approximately the time it takes the neutron to cross the nucleus.

In a compound nuclear scattering, the incident neutron loses energy upon colliding with the nucleus and is trapped. After a fairly long interval, enough energy is again concentrated on one neutron to allow it to escape.

Formalities

To formally separate the direct and compound nucleu contributions, we assume that we can partition the space of states into two components:

P -- containing the continuum states, such as the n + ^{58}Ni ones, and

Q -- containing the quasi-bound states, such as the ground and excited states of ^{59}Ni (and any other states that we don't want in P).

We define projection operators, P and Q, onto the subspaces with the properties

$$P^\dagger = P \qquad Q^\dagger = Q,$$
$$P^2 = P \qquad Q^2 = Q,$$
$$P + Q = 1$$

We then decompose the wave function into $\Psi = P\Psi + Q\Psi$, where $P\Psi$ is the continuum component and $Q\Psi$ the quasi-bound component of the wave function.

Energy averaging and the optical model

The energy average of the P-subspace wave function yields the optical wave function and scattering amplitude, which describe the fast contribution to the scattering. After rewriting the expression for the wave function in the form of an equation, we obtain an expression for the optical potential.

The energy average of the P-subspace wave function may be written directly,

$$\left\langle P\Psi_c \right\rangle = \phi_c^{(+)} + (E^{(+)} - H_{PP})^{-1} V_{PQ} \left\langle 1/e_{QQ} \right\rangle V_{QP} \phi_c^{(+)}.$$

since the only rapidly varying quantity in the wave function is

$$e_{QQ} = E - H_{QQ} - W_{QQ}.$$

By multiplying by (E-H_{PP}) as well as solving formally for $\phi_c^{(+)}$ and substituting, we can write a Schrödinger-like equation for $\langle P\Psi_c \rangle$.

,

$$\left(E - H_{PP} - V_{PQ} \frac{1}{\left\langle 1/e_{QQ} \right\rangle^{-1} + W_{QQ}} V_{QP} \right) \left\langle P\Psi_c \right\rangle = 0.$$

The optical potential, which has both real and imaginary parts, is then

$$U_{opt} = V_{PP} + V_{PQ} \frac{1}{\left\langle 1/e_{QQ} \right\rangle^{-1} + W_{QQ}} V_{QP}$$

Performing the energy average

To conclude the derivation of the optical potential, we must calculate $\langle 1/e_{QQ}\rangle$. Although there are many ways to perform the average, the simplest is to average over a normalized Lorentzian density,

$$\left\langle 1/e_{QQ}\right\rangle = \int dE_0 \, \frac{\rho(E,E_0)}{E_0 - H_{QQ} - W_{QQ}}$$

where

$$\rho(E,E_0) = \frac{\Delta}{2\pi}\frac{1}{(E-E_0)^2 + \Delta^2/4}.$$

Assuming that $1/e_{QQ}$ has no poles in the upper half of the complex E plane (causality), we can perform the integral by closing the contour in the UHP to find

$$\left\langle 1/e_{QQ}\right\rangle = (E + i\Delta/2 - H_{QQ} - W_{QQ})^{-1}$$

so that

$$U_{opt} = V_{PP} + V_{PQ}\frac{1}{E - H_{QQ} + i\Delta/2}V_{QP}$$

The optical potential is energy-dependent, non-local and complex. Its imaginary part is negative, resulting in a potential that is absorptive. The absorption accounts for the flux that is lost to the Q-subspace.

Experimental significance

An optical model calculation furnishes a wave function and a scattering amplitude that should describe the prompt part of the scattering. The S-matrix that results is an energy-averaged one. We could write the S-matrix before averaging as

$$\mathsf{S}_0 = S_0 + S_{0,fluc}, \quad \text{with} \quad \langle S_{0,fluc} \rangle = 0, \quad \text{so that} \quad \langle \mathsf{S}_0 \rangle = \langle S_0 \rangle.$$

The energy-averaged total cross-section is just the optical one,

$$\sigma_{tot} = \frac{2\pi}{k^2}\left(1 - \mathrm{Re}\langle \mathsf{S}_0 \rangle\right) = \frac{2\pi}{k^2}\left(1 - \mathrm{Re}\, S_0\right),$$

since it is linear in the S-matrix.

However, the energy-averaged elastic and absorption cross sections are

$$\sigma_{el} = \frac{\pi}{k^2}\left\langle \left|\mathsf{S}_0 - 1\right|^2 \right\rangle = \frac{\pi}{k^2}\left|S_0 - 1\right|^2 + \frac{\pi}{k^2}\left\langle \left|S_{0,fluc}\right|^2 \right\rangle$$

and

$$\sigma_{abs} = \frac{\pi}{k^2}\left\langle 1 - \left|\mathsf{S}_0\right|^2 \right\rangle = \frac{\pi}{k^2}\left(1 - \left|S_0\right|^2\right) - \frac{\pi}{k^2}\left\langle \left|S_{0,fluc}\right|^2 \right\rangle.$$

Only the total optical cross section may be compared with the experimental one.

The s-wave strength function

If we average the resonance expression for the elastic S-matrix,

$$S_{0,aa} = e^{-2i\phi_a}\left(1 - i\sum_{\mu}\frac{\Gamma_{\mu a}}{E-\varepsilon_{\mu}+i\Gamma_{\mu}/2}\right), \qquad \text{where} \quad \Gamma_{\mu a} = g_{\mu a}^2,$$

over the Lorentzian that was used to obtain the optical potential, we find

$$\overline{S}_{0,aa} = e^{-2i\phi_a}\left(1 - i\sum_{\mu}\frac{\Gamma_{\mu a}}{E-\varepsilon_{\mu}+i\Delta}\right) \approx e^{-2i\phi_a}\left(1 - \frac{\pi\overline{\Gamma}_n}{D}\right),$$

where $\overline{\Gamma}_n$ is the average neutron width and D the average s-wave resonance spacing. Since the average is the same as that of the optical potential, the average S-matrix should be the same as the optical one. In particular, we expect

$$1 - \left|S_0\right|^2 \approx 2\pi\frac{\overline{\Gamma}_n}{D}$$

when $\overline{\Gamma}_n << D$. We define the strength function as

$$s_0 = \frac{\overline{\Gamma}_n}{D}\left(\frac{E_0}{E_{cm}}\right)^{1/2} \approx \frac{1}{2\pi}\left(\frac{E_0}{E_{cm}}\right)^{1/2}\left(1 - \left|S_0\right|^2\right)$$

where E_0 is usually taken to be 1 eV. The factor of $\sqrt{E_{cm}}$ cancels the energy dependence of the neutron partial width.

Strength functions and SPRT

The s-wave strength function may be obtained from experimental data, either from measurements of the total cross section or from averages over resonances. When compared to optical model calculations, the agreement is quite good. The two peaks in the s-wave strength function occur in the regions where the 3s1/2 and 4s1/2 neutron shell-model orbitals are becoming bound and have a large overlap with continuum states.

A p-wave strength function may also be associated with p-wave absorption and extracted from data. The two strength functions, together with the scattering radius and the total cross section, may be used to fit optical model parameters at low energy. This is known as the SPRT method.

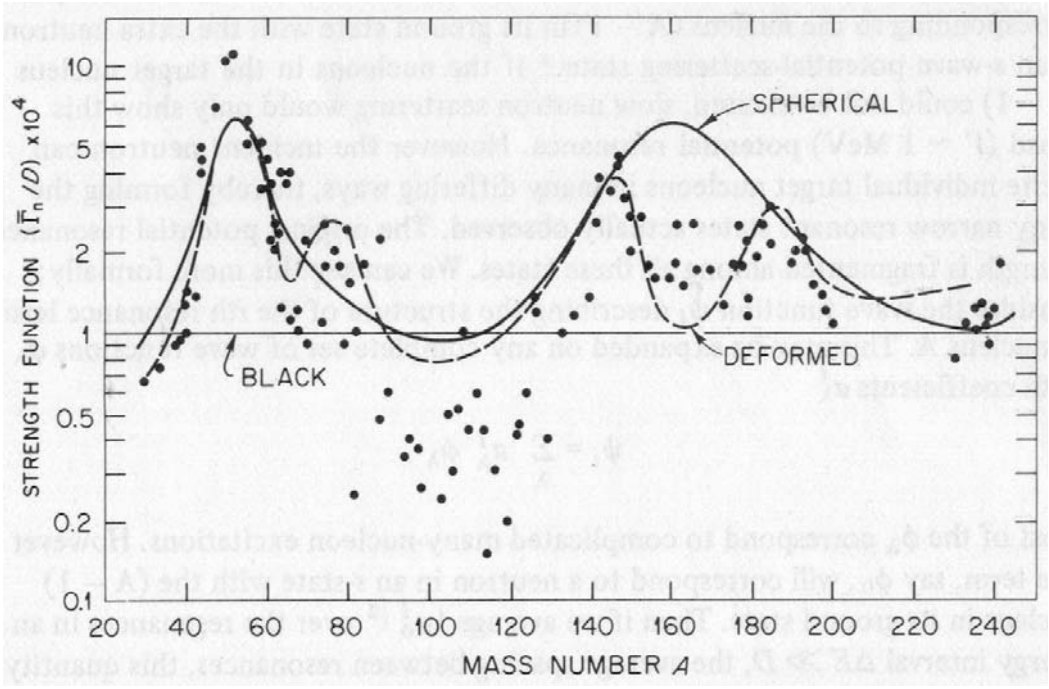

Higher partial waves

The angular distribution for a pure s-wave is obviously constant. As the energy increases, more partial waves participate in the scattering and the angular distribution becomes more forward peaked.

The highest partial wave contributing to the scattering may be crudely estimated as $l_{max} \approx kR$. For n+^{238}U at an energy of 1 MeV, this gives $l_{max} \approx 1.6$.

An important auxiliary quantity determined in an optical model calculation is the transmission coefficient, $T_l = 1 - |S_l|^2$, which is used to calculate the fluctuating contribution to the cross sections. The transmission coefficient measures the fraction of flux that is absorbed from each partial wave.

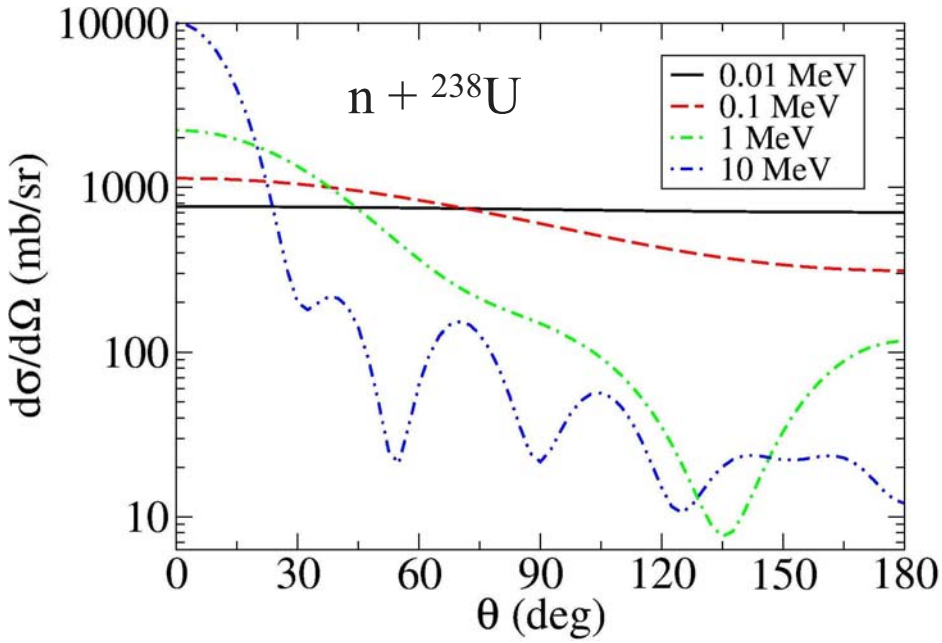

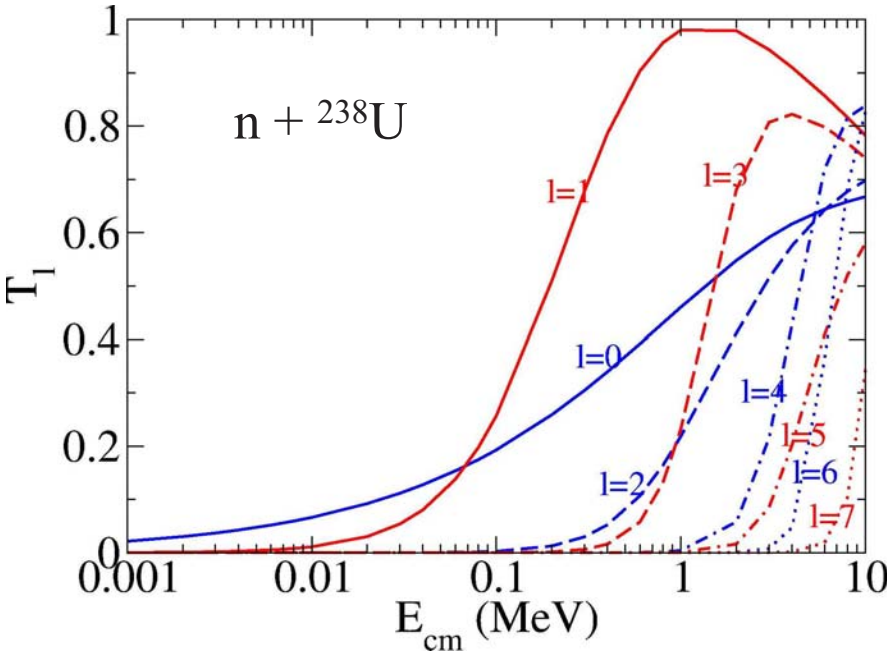

Coulomb scattering from a charge distribution

In scattering calculations, the nuclear charge distribution is usually taken as that of a uniformly charged sphere of radius R_c=1.25*A$^{1/3}$ (fm).

$$V_C(r) = \begin{cases} \dfrac{Z_P Z_T e^2}{2R_C}\left(3-(r/R_C)^2\right) & r < R_C \\ \dfrac{Z_P Z_T e^2}{r} & r > R_C \end{cases}$$

Since the nuclear potential is short-ranged, the scattering at large values of the impact parameter is Coulomb scattering.

In the example given here, the scattering at angles below about 95° would be pure point-like Coulomb scattering.

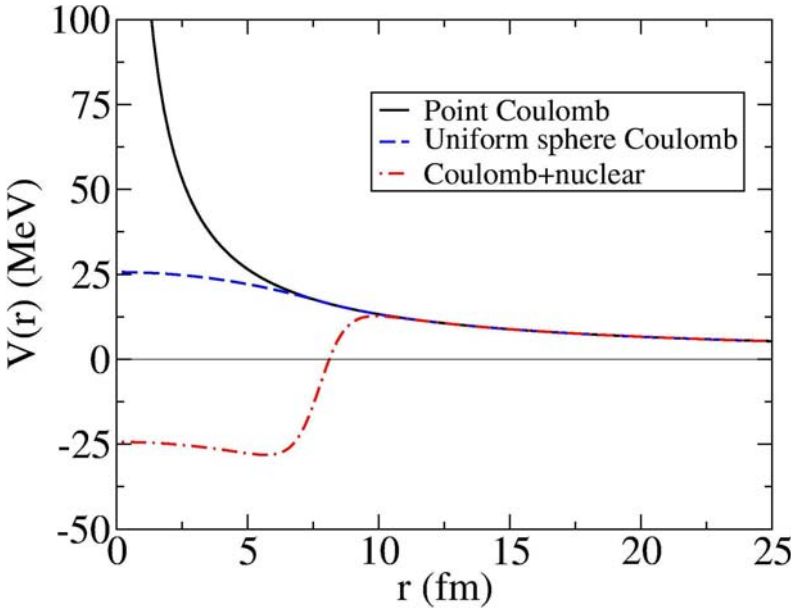

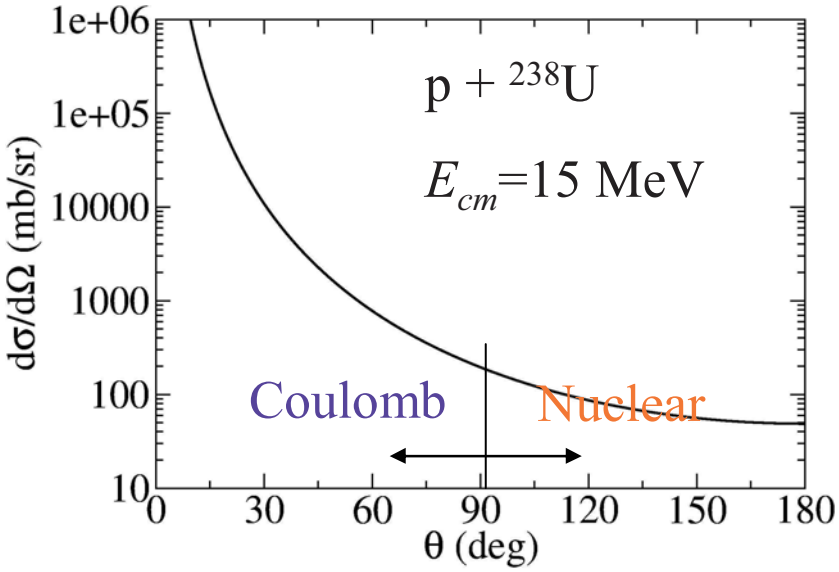

The partial wave expansion for charged particles

The difference between the partial wave expansion for neutral and charged particles is the long-range Coulomb potential. Rather than consider a plane wave, one must consider a Coulomb wave, which contains an additional logarithmic phase. The wave function can be expanded as

$$\psi_c = \frac{1}{kr}\sum_{l=0}^{\infty}(2l+1)i^l e^{i\sigma_l} F_l(kr) P_l(\cos\theta),$$

with

$$F_l(kr) = \frac{i}{2}\left(e^{-i\sigma_l} H_l^{(-)}(kr) - e^{i\sigma_l} H_l^{(+)}(kr)\right)$$

where the σ_l are the Coulomb phase shifts and

$$H_l^{(\pm)}(kr) \xrightarrow[r\to\infty]{} (\mp i)^l\, e^{\pm i(kr-\eta\ln 2kr)} \quad \text{with} \quad \eta = ka_0.$$

One may proceed as before to extract the scattering amplitude as

$$f(\theta) = f_C(\theta) + \frac{1}{2ik}\sum_{l=0}^{\infty}(2l+1)e^{2i\sigma_l}\left(S_l - 1\right)P_l(\cos\theta).$$

where

$$f_C(\theta) = -\frac{\eta}{2k\sin^2\theta/2}\exp\left[-i\eta\ln\left(\sin^2\theta/2\right) + 2i\sigma_0\right].$$

The quantum Coulomb scattering cross section is identical to the classical one.

Proton scattering

The angular distribution for proton scattering on ^{58}Ni at 1 MeV is a pure Coulomb one. Even at 4 MeV, the difference from the pure Coulomb angular distribution appears small. At 10 MeV, substantial deviations have appeared.

Nuclear effects are more easily distinguished in the transmission coefficients. They support the observation that the scattering is purely Coulomb at 1 MeV. However, at 4 MeV, 40% of the s-wave and about 10% of the p- and d-wave have been absorbed. Angular momenta through l=4 contribute at 10 MeV.

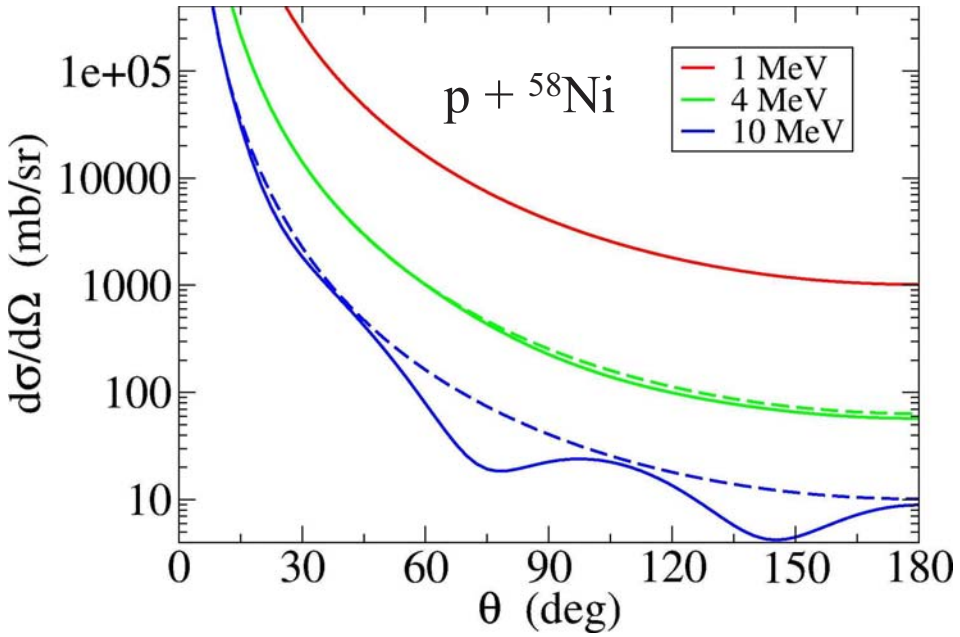

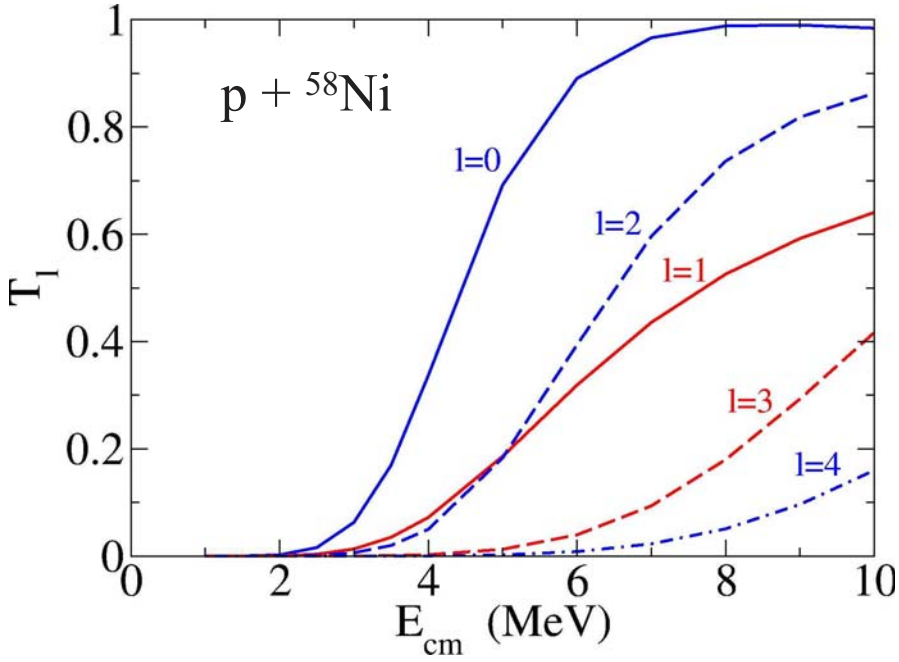

Absorption Cross sections

The absorption cross section,

$$\sigma_{abs} = \frac{\pi}{k^2}\sum_{l=0}^{\infty}(2l+1)\left(1-\left|S_l\right|^2\right)$$

$$= \frac{\pi}{k^2}\sum_{l=0}^{\infty}(2l+1)T_l,$$

takes into account the loss of flux in all partial waves.

Note the very different behavior of the absorption cross section at low energy for charged and uncharged particles. The Coulomb barrier prevents the projectile and target from reaching the region of strong interaction at low energies.

At high energies, the neutron and proton absrption cross sections tend to similar values.

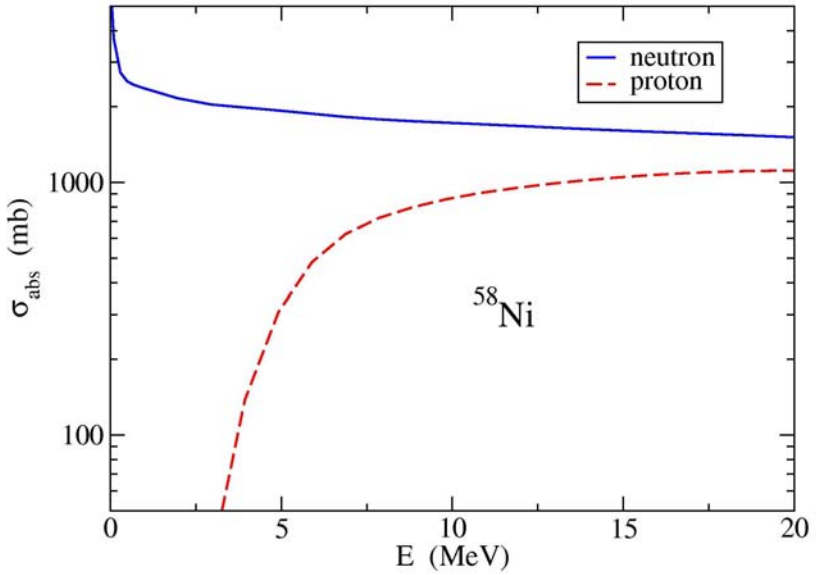

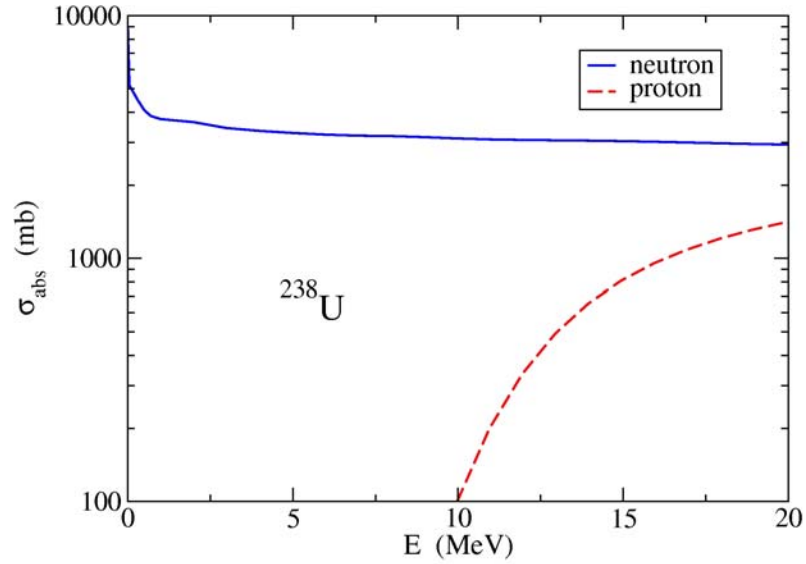

The optical potential

We obtained a formal expression for the optical potential,

$$U_{opt} = V_{PP} + V_{PQ} \frac{1}{E - H_{QQ} + i\Delta/2} V_{QP}$$

by rewriting the energy-average of the continuum component of the wave function as an equation for itself. We observed that this potential is complex, non-local and energy-dependent.

A good deal of work has been done to calculate the optical potential from first principles. These potentials are usually non-local, except at very high energies, which tends to complicate their use.

Phenomenological optical potentials are normally used to fit and compare with experimental data. These potentials are usually taken to be local. However, their geometrical characteristics and the general trend of their energy dependence are quite similar to those of microscopic potentials. They can furnish insight into what one should expect of a microscopic potential. After all, both potentials are trying to describe the same physical processes.

The phenomenological optical potential

Empirical optical potentials are determined by adjusting a limited set of parameters to the data on hand. Over the years, a standard form of the potential has evolved, which permits the parametrization of the scattering of most light particles (n, p, d, t, 3He, or α) from most nuclei. This is

$$
\begin{aligned}
U_{opt}(r) = \quad & V_C(r) && \text{a Coulomb term,} \\
& -Vf_V(r) \; - \; iWf_W(r) && \text{volume terms,} \\
& +V_S g_V(r) - iW_S g_W(r) && \text{surface terms,} \\
& -d_{so}\vec{l}\cdot\vec{\sigma}\left(V_{so}h_V(r) - iW_{so}h_W(r)\right), && \text{spin-orbit terms}
\end{aligned}
$$

where the spin-orbit constant is $d_{so} = \left(\hbar / m_\pi c\right)^2 \approx 2 \text{ fm}^2$.

The Coulomb potential is usually taken to be the interaction of a point charge with a uniformly-charged sphere of radius R_c=1.25*A$^{1/3}$ (fm),

$$
V_C(r) = \begin{cases} \dfrac{Z_P Z_T e^2}{2R_C}\left(3 - (r/R_C)^2\right) & r < R_C \\ \dfrac{Z_P Z_T e^2}{r} & r > R_C \end{cases}
$$

The volume terms of the optical potential

The volume terms are usually taken to be of Wood-Saxon form,

$$f_i(r) = \frac{1}{1+\exp\left[(r-R_i)/a_i\right]} \qquad i = V, W,$$

where R_i and a_i are the radii and diffusivities of the two terms.

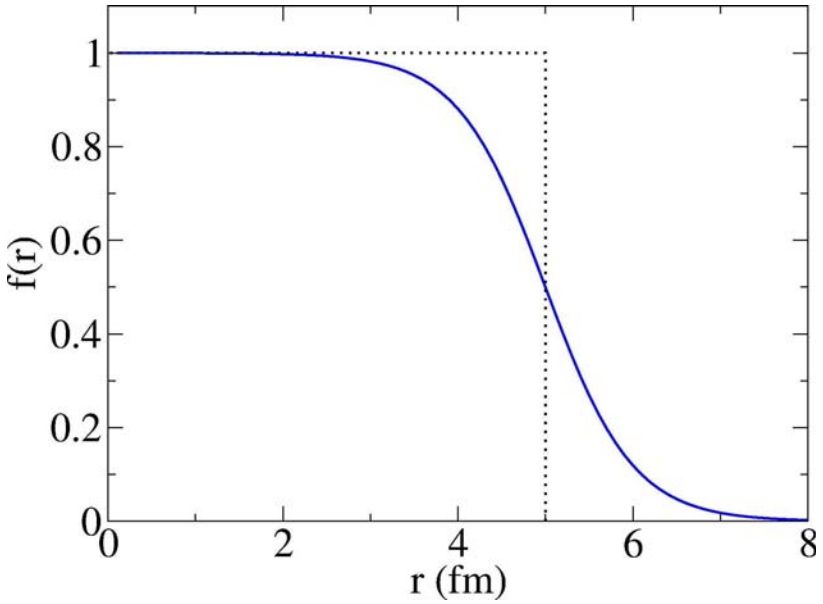

The Wood-Saxon form is quite similar to the nucleon density of a saturated nucleus (A>30).

The real volume potential reflects the average interaction of the projectile with the nucleons of the target. The strength of the real volume potential is roughly proportional to the mass of the projectile and and decreases with energy, in agreement with nuclear mean field calculations.

The imaginary volume potential takes into account the loss of projectile flux due to collisions with the nucleons in the target. It is zero at low energy, below the threshold for single-particle excitations, and increases with energy as the phase space of single-particle modes increases.

The surface terms of the optical potential

The surface terms are usually taken to be either the derivative of a Wood-Saxon,

$$g_i(r) = -4a_i \frac{d}{dr} f_i(r) = 4 \frac{\exp\left[(r-R_i)/a_i\right]}{\left(1+\exp\left[(r-R_i)/a_i\right]\right)^2} \quad i = V, W,$$

or a Gaussian,

$$g_i(r) = \exp\left[(r-R_i)^2/a_i^2\right] \quad i = V, W.$$

The two are practically indistinguishable when a_G=2.21 a_{WS}.

The imaginary surface term takes into account the absorption due to the excitation of low-energy collective modes, which have their couplings concentrated on the surface.

A real surface term can result from the same coupling but can also be explained using a dispersion relation.

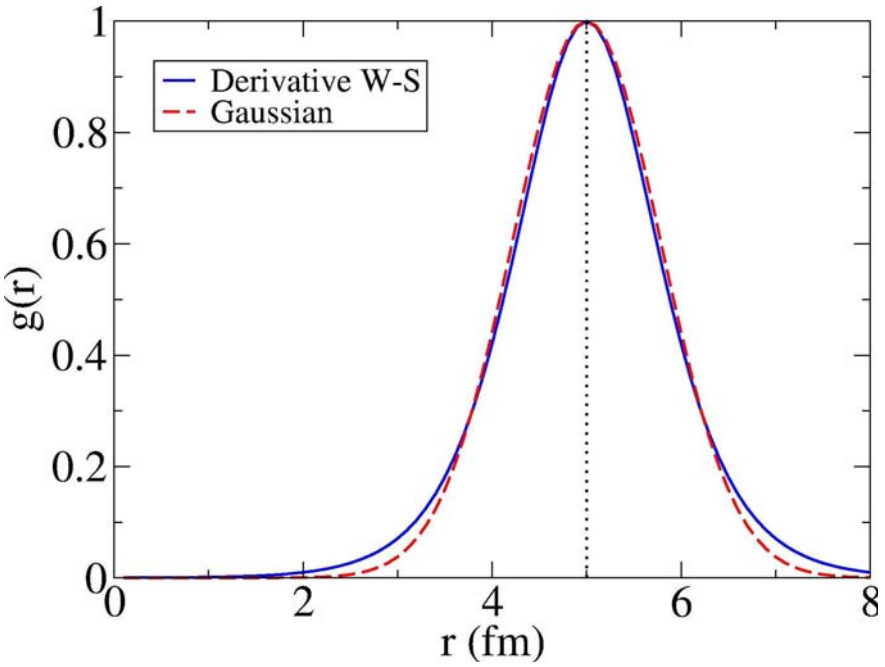

The spin-orbit terms of the optical potential

The spin-orbit terms are taken to have a Thomas form factor,

$$h_i(r) = -\frac{1}{r}\frac{d}{dr} f_i(r) = \frac{1}{r a_i} \frac{\exp\left[(r - R_i)/a_i\right]}{\left(1 + \exp\left[(r - R_i)/a_i\right]\right)^2} \qquad i = V, W.$$

The spin-orbit interaction also acts between the bound states of a nucleus, where it increases the binding of the $j=l+½$ levels and decreases the binding of the $j=l$-1/2 levels.

The Thomas form factor and the spin-orbit potential itself are obtained (for spin ½) when the Dirac equation with Wood-Saxon potentials is reduced to an equivalent Schrödinger equation. The spin-orbit interaction is thus another manifestation of the volume interaction of the projectile with the nucleons of the target.

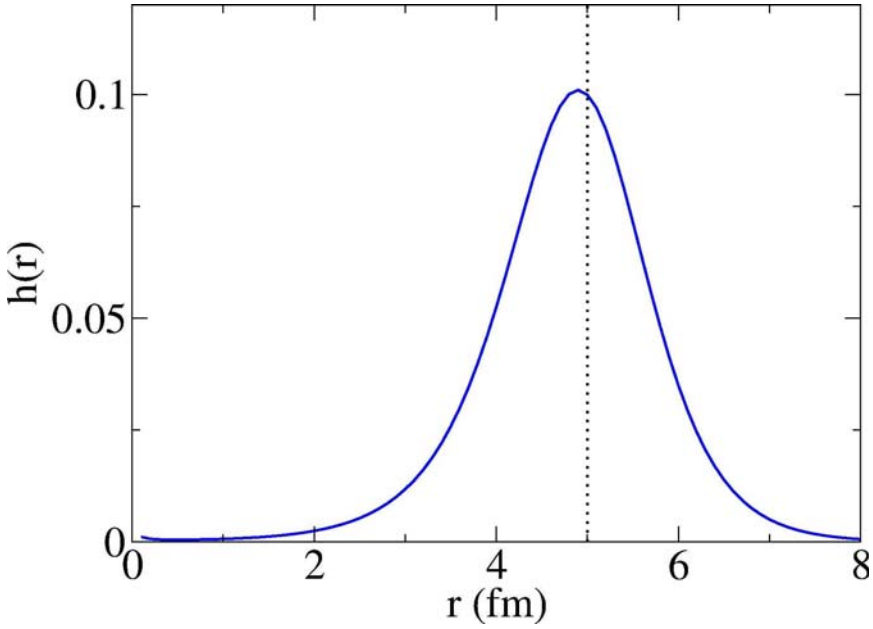

Optical potential parameters

The phenomenological optical potential is thus parametrized in terms of a set of potential strengths and corresponding geometrical parameters.

The best modern reference for optical potential parameters (for light projectiles) is the Reference Input Parameter Library (RIPL-2), available from the International Atomic Energy Agency.

For nucleons, typical values of the potential strengths are

$$V \approx (45-55)\ \text{MeV} - (0.2-0.3)E,$$

$$W_s \approx (2-7)\ \text{MeV} - (0.1-0.3)E \qquad E < 8-10\ \text{MeV},$$

$$V_{so} \approx (4-10)\ \text{MeV}.$$

Above 8-10 MeV, W_s is usually constant or slightly decreasing. V_s and W_{so} can normally be taken to be zero as can W below about 10 MeV. Above about 10 MeV, W is constant or slightly increasing.

The radii R_i take on values $R_i = r_i A_T^{1/3}$ with the reduced radii in the range $r_i \approx 1.2 - 1.3$ fm. The diffusivities are normally in the range $a_i \approx 0.4 - 0.7$ fm.

Fairly wide ranges of the parameters V, R_V, W_s and a_s result in equally good fits if VR_V^2 and $W_s a_s$ remain constant. These are called potential ambiguities.

The microscopic optical potential -- I

Microscopic optical potentials attempt to describe the projectile-target interaction in terms of nucleon-nucleon interactions, such as these representing the first few terms in nucleon-nucleus interaction.

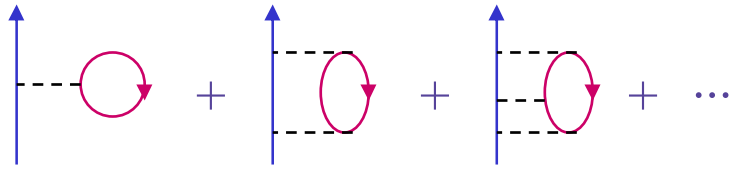

A systematic method for summing the most important terms is provided by the self-consistent Brueckner approximation. The Brueckner G-matrix is calculated by summing repeated interactions, taking into account effects of the nuclear medium.This calculation is usually performed in infinite nuclear matter, for simplicity.

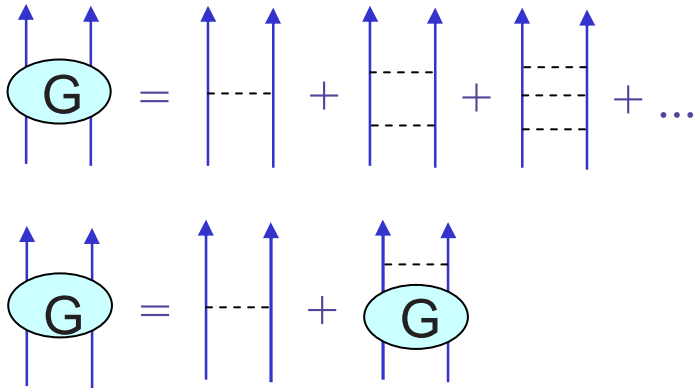

The G-matrix is then folded over the target nucleon density to obtain the optical potential *U*. Self-consistency requires that the target density be obtained with the same potential.

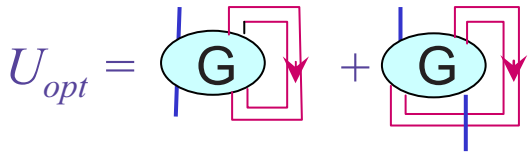

The microscopic optical potential -- II

The microscopic optical potential possesses a direct term and an exchange term. The exchange term is non-local and both are energy-dependent. The exchange term is often approximated as a local term with an additional energy-dependence (JLM).

U_{opt} = G + G

= U_d + U_{ex}

At high energy, the microscopic optical potential reduces to the impulse approximation potential, obtained by folding the two-nucleon *t*-matrix with the target density -- the *t*ρ approximation.

The figure compares experimental reaction cross sections for ^{12}C, ^{28}Si, ^{56}Fe ^{90}Zr and ^{208}Pb, in ascending order, with microscopic optical model calculations by Amos and Karataglidis.

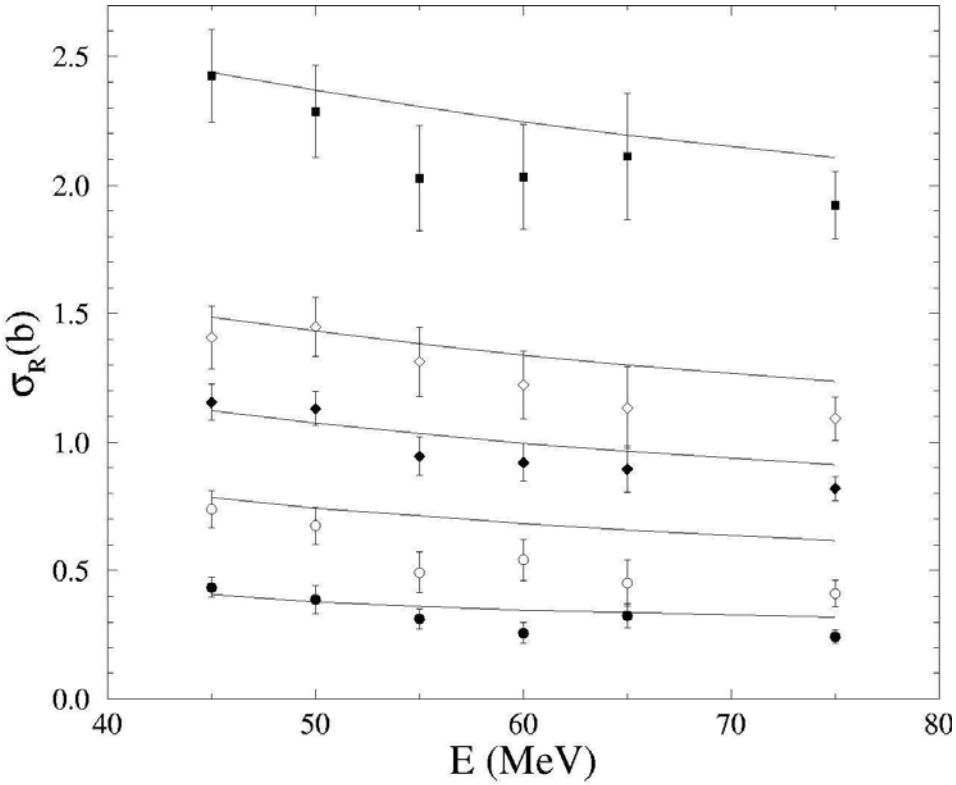

The optical potential at low energy

Formally, we derived the optical potential by considering the scattering in a subspace P of the space of states and then energy-averaged to smooth the dependence on the remaining subspace of states Q. We obtained

$$U_{opt} = V_{PP} + V_{PQ} \frac{1}{E - H_{QQ} + i\Delta/2} V_{QP}.$$

In the microscopic optical potential, the division into P and Q subspaces is no longer transparent. It is there, contained in the G-matrix, but in terms of nucleon-nucleon scattering rather than nucleon-nucleus scattering. We would thus expect that the microscopic potential does not take into account the collective effects that are often important at low energies. We might consider decomposing the optical potential at low energies (using a local approximation) as

$$U_{opt}(r,E) = U_{sp}(r,E) + U_{coll}(r,E),$$

where U_{sp} is the microscopic potential and U_{coll} is the remainder, which we might attribute to collective effects. At low energies, $U_{sp}(r,E) \approx V_{HF}(r,E)$. At high energy, we expect that $U_{coll}(r,E) \to 0$.

Dispersion relations

Because of causality, the optical potential should have no singularities in the upper half-energy plane. We may then write

$$\int dE' \frac{U_{coll}(r,E')}{E'-E} = 0,$$

which we may rewrite as

$$\text{P.P.} \int dE' \frac{U_{coll}(r,E')}{E'-E} = i\pi U_{coll}(r,E)$$

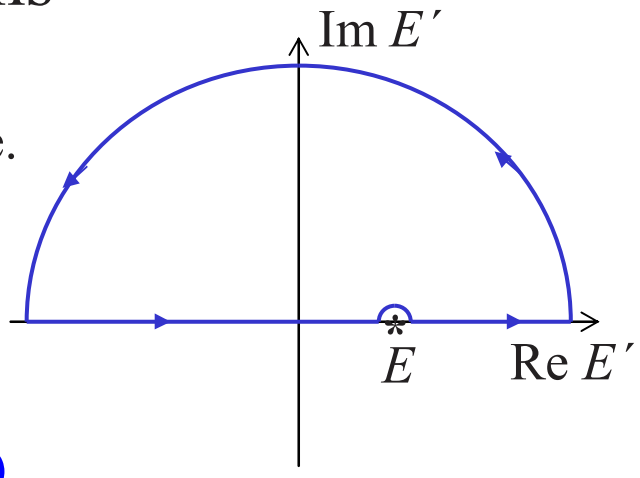

Separating U_{coll} into its real and imaginary parts, $U_{coll} = \Delta V + i\,W$, we have

$$\Delta V(r,E) = \text{P.P.} \frac{1}{\pi} \int dE' \frac{W(r,E')}{E'-E}$$

At low energy, $U_{opt} \approx V_{HF} + \Delta V + i\,W.$

The effect of ΔV is seen as a strengthening in the real part of the optical potential at low energy relative to the linear dependence expected of V_{HF}.

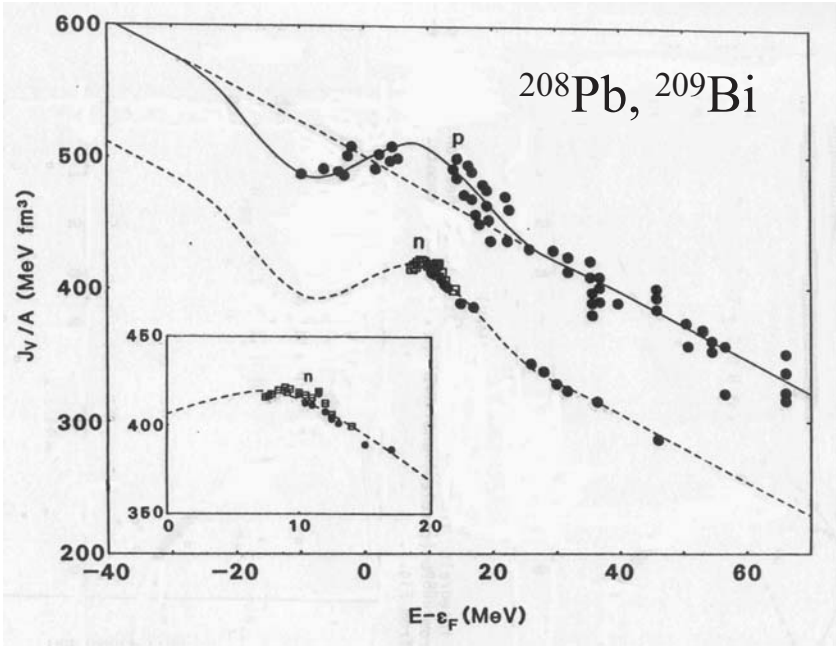

(Finlay and Petler, Opt. Model 1986)

The single-channel optical model -- spin

Because of the spin-orbit interaction, a rigorous treatment of neutron or proton scattering requires that the spin be included in the calculation. To do this, one performs the partial wave expansion of the scattering wave function (spin s) as

$$\Psi = \frac{4\pi}{kr}\sum_{ljn} i^l e^{i\sigma_l}\psi_l^j(r)\mathcal{Y}_{ls}^{jn}(\hat{r})\mathcal{Y}_{ls}^{jn\dagger}(\hat{k}),$$

in terms of the spin-angular functions,

$$\mathcal{Y}_{ls}^{jn}(\hat{r}) = i^l\sum_{m\nu}\left\langle lms\nu \middle| j\,n\right\rangle Y_{lm}(\hat{r})\left|s\nu\right\rangle,$$

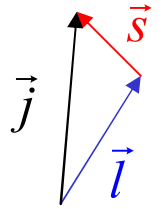

where l and j are the orbital and total angular momenta and $|s\nu\rangle$ is a spin eigenvector. In the expansion, σ_l is the Coulomb phase shift, $\hat{r}$ denotes the angular variables and $\hat{k}$ the direction of the incident momentum. The spin-angular functions are vectors with components labeled by ν, the projection of the spin.

Because of angular momentum and parity conservation, the equations for the $\psi_l^j(r)$ uncouple. They can then be solved as before and the asymptotic behavior of the resulting wave function analyzed to extract the scattering amplitude.

The scattering amplitude -- spin

The scattering amplitude

$$f(\theta) = f_C(\theta)\mathbf{1} + \frac{4\pi}{2ik}\sum_{ljn} e^{2i\sigma_l}\left(S_l^j - 1\right)\mathrm{Y}_{ls}^{jn}(\hat{r})\mathrm{Y}_{ls}^{jn\dagger}(\hat{k}),$$

with $f_C(\theta)$ the Coulomb scattering amplitude, is now a matrix, $f_{\nu\nu'}(\theta)$, with matrix elements labeled by the spin projections ν and ν'.

For particles of spin ½,

$$f(\theta) = \begin{pmatrix} A(\theta) & B(\theta) \\ B(\theta) & A(\theta) \end{pmatrix}$$

where

$$A(\theta) = f_C(\theta) + \frac{1}{2ik}\sum_l e^{2i\sigma_l}\left[(l+1)\left(S_l^{l+1/2} - 1\right) + l\left(S_l^{l-1/2} - 1\right)\right]P_l(\cos\theta),$$

and

$$B(\theta) = \frac{1}{2ik}\sum_l e^{2i\sigma_l}\left[S_l^{l+1/2} - S_l^{l-1/2}\right]P_l^1(\cos\theta).$$

The amplitude *A* corresponds to scattering in which the spin projection remains constant. The amplitude *B* describes scattering in which the spin projection flips.

A: ↑ ➡ ↑ ↓ ➡ ↓ *B*: ↑ ➡ ↓ ↓ ➡ ↑

Angular distributions -- spin

The differential elastic cross section for an unpolarized incident beam is obtained by averaging the squared magnitudes of the scattering amplitudes over the initial values of the projectile spin and summing over the final ones,

$$\frac{d\sigma}{d\Omega} = \frac{1}{2s+1}\sum_{\nu\nu'}\left|f_{\nu'\nu}(\theta)\right|^2 .$$

For spin-1/2 particles, this becomes

$$\frac{d\sigma}{d\Omega} = \left|A(\theta)\right|^2 + \left|B(\theta)\right|^2 \qquad s = 1/2.$$

For particles of spin ½ and greater, vector and possibly tensor spin observables may be defined in terms of other combinations of the amplitudes. For particles of spin ½, the vector polarization $P(\theta)$ and the spin rotation function $Q(\theta)$ are defined as

$$P(\theta) = \frac{2\,\mathrm{Im}\,A^*(\theta)B(\theta)}{d\sigma/d\Omega} \qquad \text{and} \qquad Q(\theta) = \frac{2\,\mathrm{Re}\,A^*(\theta)B(\theta)}{d\sigma/d\Omega}.$$

Polarization in neutron scattering

The spin-summed angular distribution due to scattering of a polarized beam may be written as

$$\frac{d\sigma_{pol}}{d\Omega} = \frac{d\sigma}{d\Omega}\left(1 + P(\theta)\,\hat{n}\cdot\vec{P}_{pol}\right),$$

where $\vec{P}_{pol}$ is a vector defining the intitial polarization and $\hat{n}$ is the normal to the scattering plane.

The spin-orbit interaction is fairly strong. Its effects on the polarization become visible as soon as partial waves above the s-wave contribute to the scattering.

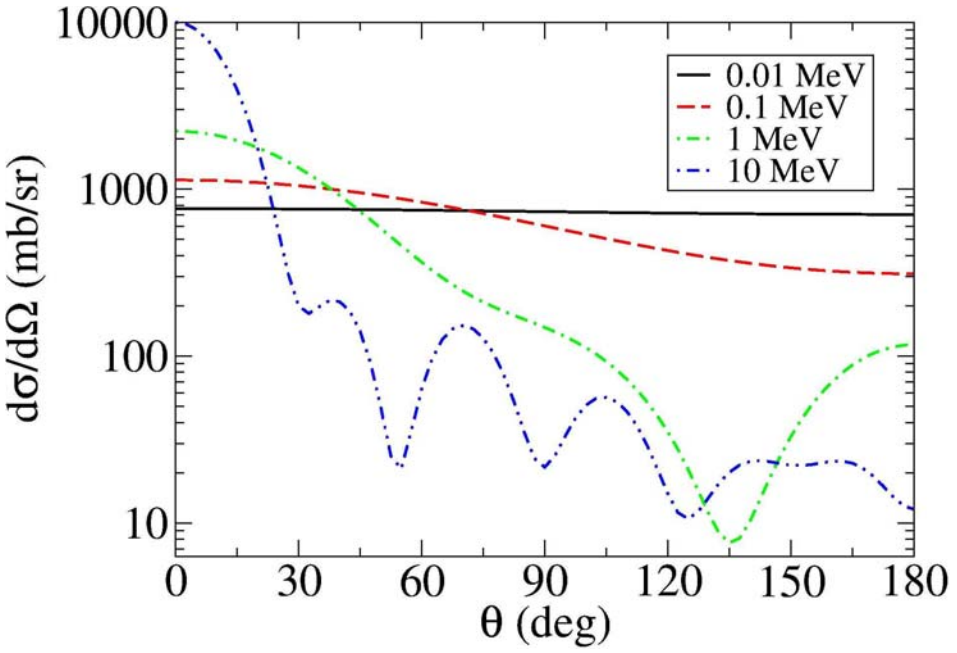

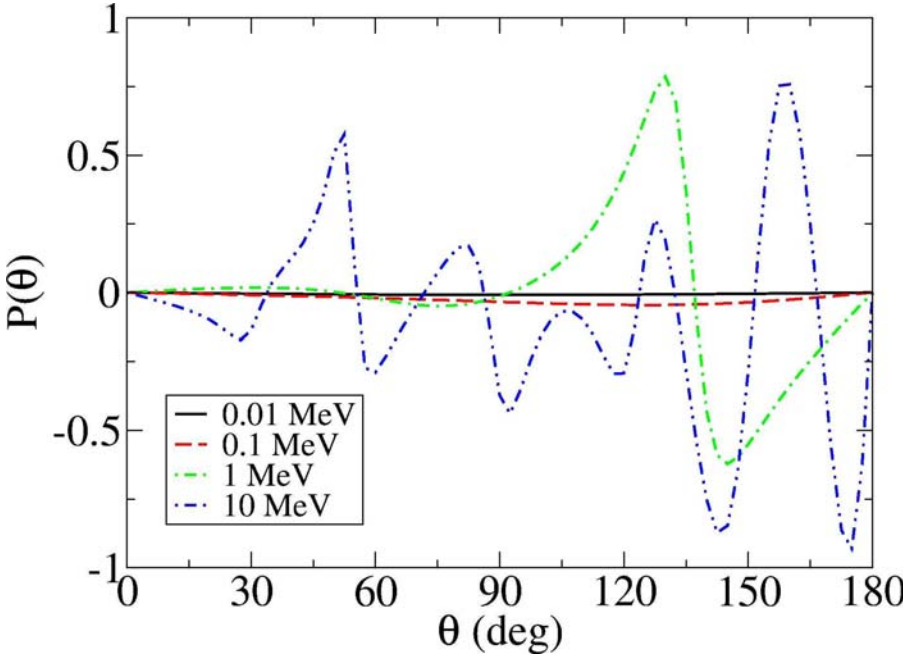

Integrated cross sections -- spin

As before, the absorption cross section may be related to flux lost from the asymptotic probability current density,

$$\sigma_{abs} = -\frac{1}{v}\int_S \vec{j}\cdot d\vec{S} = \frac{1}{2s+1}\frac{\pi}{k^2}\sum_{lj}(2j+1)\left(1-\left|S_l^j\right|^2\right).$$

The fraction of the flux lost from each partial wave may also be expressed as a transmission coefficient,

$$T_l^j = 1-\left|S_l^j\right|^2.$$

For charged particles, the Coulomb interaction leads to an infinite elastic cross section. For neutrons, integration of the differential cross section yields

$$\sigma_{el} = \int d\Omega \frac{d\sigma}{d\Omega} = \frac{\pi}{2k^2}\sum_{lj}(2j+1)\left|S_l^j - 1\right|^2.$$

For neutron, the total cross section may be defined as the sum of the elastic and absorption ones,

$$\sigma_{tot} = \sigma_{el} + \sigma_{abs} = \frac{\pi}{k^2}\sum_{lj}^{\infty}(2j+1)\left(1-\mathrm{Re}\,S_l^j\right).$$

Comparison with experiment

We recall that, being linear in the scattering amplitude, the total optical cross section may be compare to the energy-averaged experimental one. We see that reasonable agreement with the data is possible here.

We also verified that the partial wave contributions to the energy-averaged elastic cross section,

$$\sigma^{j}_{l,el} = \frac{\pi}{k^2}\left|S^{j}_{l} - 1\right|^2 + \frac{\pi}{k^2}\left\langle \left|S^{j}_{l,fluc}\right|^2 \right\rangle$$

exceed the shape elastic (optical) ones due to contributions from fluctuations. We observe that the fluctuation contributions are negligible only at higher energies.

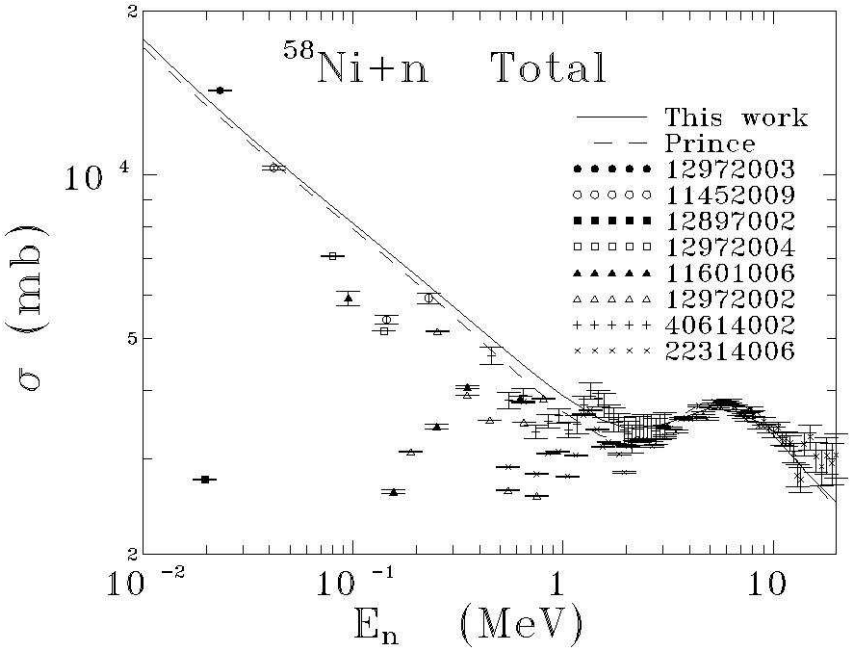

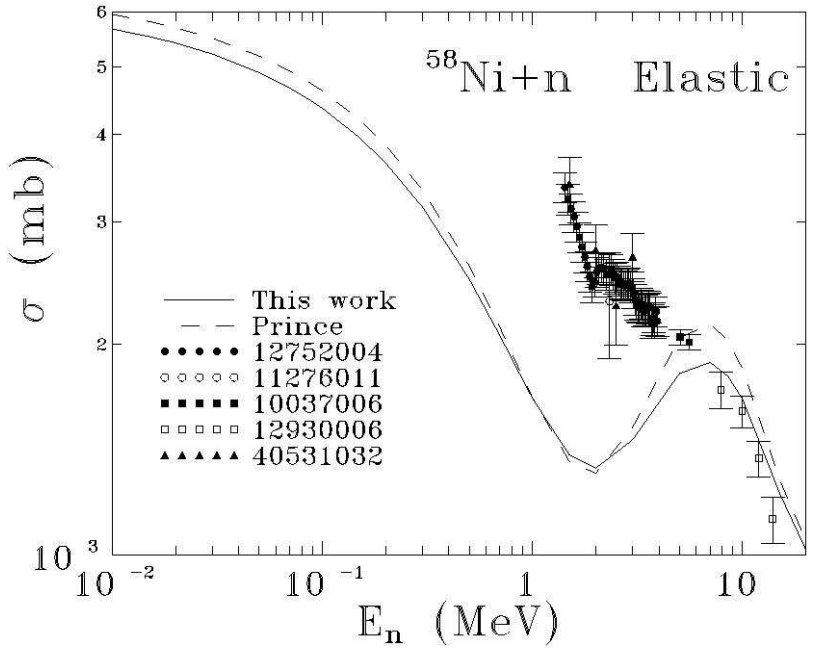

Inelastic scattering

The single-channel optical model describes the scattering in the elastic channel alone. It is often called the spherical optical model because, in it, the target may be considered to be spherically symmetric since its structure is never introduced.

Direct reactions that transfer energy as well as momentum are often important. Such inelastic scatterings, in the case of inert projectiles (n, p, α, d, etc.), leave the target in an excited state and diminish the asymptotic kinetic energy of the projectile. In heavy ion collisions, both the projectile and the target are sometimes excited. To describe inelastic scattering, we must introduce at least the basic characteristics of the ground and excites states of the target and/or projectile.

The nature of the ground and excited states of a nucleus are also important factors in detemining the degree to which it is excited in a collision. The states that are most strongly excited in collisions are those that involve collective movement, vibrations and rotations, in particular.

Vibrations

Every nucleus possesses collective vibrational modes of excitation. Their importance in low-energy scattering, however, varies greatly from nucleus to nucleus.

Vibrational modes may be understood qualitatively as shape oscillations of intermixed but incompressible neutron and proton fluids about their equilibrium configuration. The protons and neutrons may oscillate in phase (isoscalar) or out of phase (isovector) with one another.

The simplest modes are:

	Isoscalar	Isovector
$l=1^-$ – dipole	CM displacement	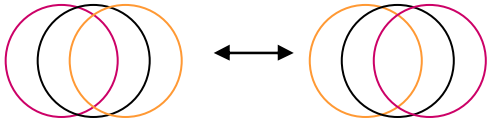
$l=2^+$ -- quadrupole	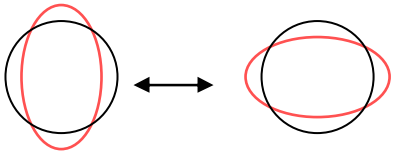	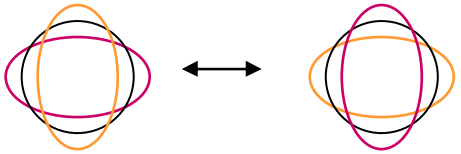

Octupole ($l=3^-$) modes are also common and many others have been observed.

Vibrations – Excitation Energies and states

Isovector vibrations occur at higher energies than the corresponding isoscalar ones, because of the strong nuclear attraction between protons and neutrons.

Negative parity vibrational modes tend to vary smoothly in energy as a function of the mass number. Positive parity vibrational modes, vary greatly with the mass and depend on the shell structure. The variations in the excitation energies are explained in a microscopic treatment in terms of particle-hole pairs:

Negative parity – particle-hole pairs from two adjacent shells,

Positive parity – particle-hole pairs from same shell, when possible,
otherwise from one shell and from second higher shell.

Ex.: ^{208}Pb – the first excited state is the 3^- octupole state.

Vibrations are bosonic modes. Multiple excitations are possible but must form symmetric states. Thus an excited state consisting of two $l=2^+$ quadrupole phonons on a $I=0^+$ ground state may have $I=0^+,2^+, 4^+$.

The states may be written in terms of creation operators $b^\dagger_{I_c N_c}$ as

$$\left|cI_cN_c\right\rangle = b^\dagger_{I_cN_c}\left|0\right\rangle \qquad \text{and} \qquad \left|c_1c_2I_cN_c\right\rangle = \frac{1}{\sqrt{1+\delta_{I_1I_2}}}\left[b^\dagger_{I_1}b^\dagger_{I_2}\right]_{I_cN_c}\left|0\right\rangle$$

Vibrations – An example

In the simplest case of non-interacting phonons, the spectrum is harmonic. The ideal spectrum of the first few excited quadrupole states on an $I=0^+$ ground state are shown here.

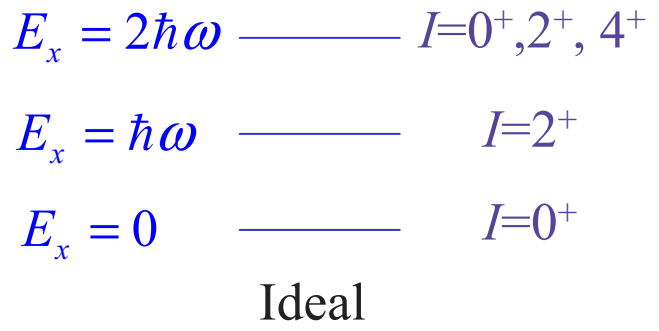

We compare this with the first few excited states of ^{58}Ni (energies in MeV).

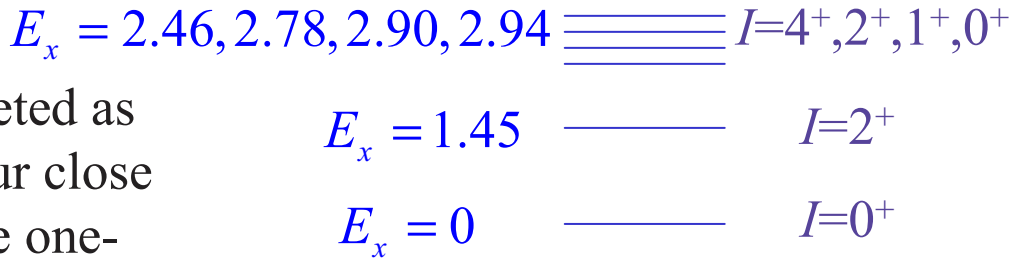

The three states that can be interpreted as two-phonon quadrupole states occur close in energy to twice the energy of the one-phonon state and have the correct spin and parity The 1^+ state, however, does not.

Another indicator of the relationship between the states are the branching ratios for their EM decay. The two-phonon 4^+ and 2^+ states decay almost exclusively to the one-phonon 2^+ state, as does the 1^+ state. The 0^+ state decays to several of the others, but principally to the 1^+ state.

Rotations

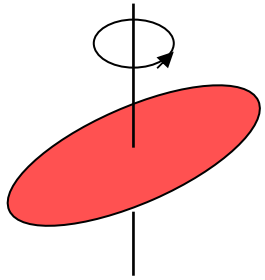

Many nuclei in the regions between closed shells possess a statically deformed ground state with axial symmetry. The lowest energy excited states of these nuclei are usually rotations about an axis perpendicular to the symmetry axis.

We can approximate the surface of a deformed nucleus as

$$R(\theta') = R_0\left(1+\sum_{\lambda}\beta_\lambda Y_{\lambda 0}(\theta')\right),$$

where the β_λ, λ=2, 4, 6,... are deformation parameters and the angle θ' is taken with respect to the symmetry axis of the nucleus. The most important of the deformation parameters is β_2.

When β_2 <0, the nucleus is oblate. When β_2 >0, the nucleus is prolate.

The wave function of a rotational state can be written in terms of an intrinsic wave function χ_K and the rotation matrices D^I_{NK} as

$$\left\langle \vec{r}_{\text{int}} \left| cI_cN_c \right\rangle = \frac{1}{\sqrt{1+\delta_{K0}}}\sqrt{\frac{2I_c+1}{16\pi^2}}\left[\chi_K(\vec{r}_{\text{int}})D^{I_c*}_{N_cK}(\hat{r}_{\text{int}})+(-)^{I_c-I_\chi}\chi_{-K}(\vec{r}_{\text{int}})D^{I_c*}_{N_c,-K}(\hat{r}_{\text{int}})\right]\right.$$

where K is the projection of the angular momentum on the symmetry axis.

Rotations – An example

A rotational band built on a 0^+ ground state consists of states with $I=0^+, 2^+, 4^+, 6^+, \ldots$ A rotational band built on a ground state with spin $I_0 \neq 0$ consists of states with $J=I_0, I_0+1, I_0+2, I_0+3, \ldots$

The excitation energy of a state with angular momentum I is

$$E_x(I) = \frac{\hbar^2}{2\mathcal{I}}\left[I(I+1) - I_0(I_0+1)\right].$$

The nucleus ^{238}U possesses static deformations of $\beta_2=0.198$ and $\beta_4=0.057$. The rotational band based on its 0+ ground state consists of excited states with

$I=2^+$ $E_x=0.045$ MeV = 0.0075 MeV * 2*3,
$I=4^+$ $E_x=0.148$ MeV = 0.0074 MeV * 4*5,
$I=6^+$ $E_x=0.307$ MeV = 0.0073 MeV * 6*7,
$I=8^+$ $E_x=0.518$ MeV = 0.0072 MeV * 8*9,
:
$I=28^+$ $E_x=4.516$ MeV = 0.0056 MeV *28*29, and possibly more.

The electromagnetic decay of each of these states occurs exclusively to the next state of lower energy in the chain.

The generalized optical potential -- vibrations

The simplest manner of extending the optical potential to take into account either static deformation or the dynamical deformation of a vibrational mode is to modify the radii of the terms in the potential accordingly.

In its simplest form, a vibrational mode of a nucleus may be taken as a shape oscillation about a spherical equilibrium mode. The radii of the terms in the potential may be expressed as

$$R_i = R_{0i}\left(1+\sum_{\lambda\mu} a_{\lambda\mu} Y_{\lambda\mu}(\hat{r})\right), \qquad \text{with} \qquad a_{\lambda\mu} = \frac{\beta_\lambda}{\sqrt{2\lambda+1}}\left(b^\dagger_{\lambda\mu} + (-)^\mu b_{\lambda-\mu}\right),$$

where $b^\dagger_{\lambda\mu}$ and $b_{\lambda\mu}$ are the phonon creation/annihilation operators and the β_λ are the amplitudes of the shape oscillations.

We may then expand the optical potential in the creation/annihilation operators as

$$U_{opt}(\vec{r}) = U_{opt}(r) + \sum_i \frac{\partial U_{opt}}{\partial R_i} R_{0i} \sum_{\lambda\mu} a_{\lambda\mu} Y_{\lambda\mu}(\hat{r}).$$

The potential is sometimes expanded to second order in the operators. The second order potential permits single-step transitions to two-phonon states.

The generalized optical potential -- rotations

The optical potential for a deformed nucleus may also be obtained by expanding the deformed potential radii

$$R_i(\theta') = R_{0i}\left(1+\sum_\lambda \beta_\lambda Y_{\lambda 0}(\theta')\right),$$

in a Taylor series in the deformation parameters, β_λ. However, when the deformations are large, it is better to expand it directly in multipoles as

$$U_{opt}(r,\hat{r}') = \sum_\lambda U_\lambda(r) Y_{\lambda 0}(\hat{r}') \qquad \text{with} \qquad U_\lambda(r) = \int d\Omega' U_{opt}(r,\theta') Y_{\lambda 0}(\theta').$$

The moments $U_{\lambda\mu}(r)$, with $\mu \neq 0$, vanish in the body-fixed frame. The body-fixed angles $\hat{r}'$ are related to the space fixed ones $\hat{r}$ through the collective angular coordinates of the nucleus, $\hat{r}_{\text{int}}$. This implies that

$$Y_{\lambda 0}(\hat{r}') = \sum_\mu Y_{\lambda\mu}(\hat{r}) D^\lambda_{\mu 0}(\hat{r}_{int}) = \sum_\mu Y_{\lambda\mu}(\hat{r}) Y^*_{\lambda\mu}(\hat{r}_{int}).$$

The optical potential in the rotational model may thus be expanded as

$$U_{opt}(\vec{r},\hat{r}_{\text{int}}) = \sum_{\lambda\mu} U_\lambda(r) Y_{\lambda\mu}(\hat{r}) Y^*_{\lambda\mu}(\hat{r}_{\text{int}}).$$

The generalized optical potential, in both models, couples the relative motion to the internal degrees of freedom of the target.

Coupled-channels partial wave expansion

To properly take into account the angular momentum of the target, the spin-angular functions must be coupled to the target states to form target-spin-angular functions of total angular momentum J and projection M,

$$\mathcal{Y}^{JM}_{lsjc}(\hat{r}) = \sum_{nN_c} \left\langle jnI_cN_c \middle| JM \right\rangle \mathcal{Y}^{jn}_{ls}(\hat{r}) \middle| cI_cN_c \right\rangle .$$

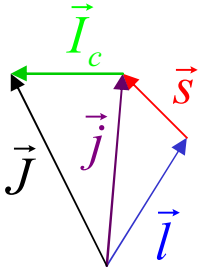

The functions also depend on the internal target coordinates. In terms of these, the scattering wave function may be expanded in a sum over both the excited states and angular momenta,

$$\Psi = 4\pi \sum_{\substack{ljcJM \\ l'j'c'}} \mathcal{Y}^{JM}_{l'sj'c'}(\hat{r}) i^{l'} \psi^{J}_{l'j'c',ljc}(r) \frac{e^{i\sigma_{lc}}}{k_c r} \mathcal{Y}^{JM\dagger}_{lsjc}(\hat{k}).$$

The most significant difference here is that the partial wave functions depend on two sets of indices, l, j, c and l', j', c'. For a particle with spin in the spherical optical model, we have two indices l and l', in principal, for each value of the total angular momentum j. For particles of spin 0 or spin ½, parity conservation reduces the two, l and l', to have the same value. The partial wave functions and S-matrix elements are then uncoupled scalar quantities. Here, we should look more carefully to see how the channels could be coupled.

Coupled partial waves

To analyze the partial waves that can couple, we must consider all possible combinations of the orbital angular momentum l, the spin s, the channel angular momentum j and the target spins I_c that can sum to a given value J of the total angular momentum and possess a given value of the parity, π.

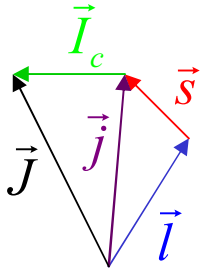

Consider a simple example: a spin-½ nucleon incident on a 0^+ ground state that can be excited to a 2^+ target state. We have

For the $J^\pi=1/2^+$ channel:

0+ ground state: l=0, j=1/2

2+ excited state: l=2, j=3/2

l=2, j=5/2

3 coupled channels

For the $J^\pi=1/2^-$ channel:

0+ ground state: l=1, j=1/2

2+ excited state: l=1, j=3/2

l=3, j=5/2

For the $J^\pi=5/2^+$ channel:

0+ ground state: l=2, j=5/2

2+ excited state: l=0, j=1/2

l=2, j=3/2

l=2, j=5/2

l=4, j=7/2

l=4, j=9/2

6 coupled channels

For the $J^\pi=5/2^-$ channel:

0+ ground state: l=3, j=5/2

2+ excited state: l=1, j=1/2

l=1, j=3/2

l=3, j=5/2

l=3, j=7/2

l=5, j=9/2

The coupled equations

When the partial-wave expansion is substituted in the Schrödinger equation, it reduces to a set of coupled equations for each value of J^π,

$$\frac{\hbar^2}{2\mu}\left\{\frac{d^2}{dr^2}-\frac{l'(l'+1)}{r^2}+k_{c'}^2\right\}\psi^J_{l'j'c',ljc}(r)-\sum_{l''j''c''}\mathsf{U}^J_{l'j'c',l''j''c''}(r)\psi^J_{l''j''c'',ljc}(r)=0,$$

where the potential matrix elements are those of the target-spin-angular functions,

$$\mathsf{U}^J_{l'j'c',ljc}(r)=\int d\Omega\ \mathsf{Y}^{JM\dagger}_{l'sj'c'}(\hat{r})U_{opt}(\vec{r},\vec{r}_{\rm int})\mathsf{Y}^{JM}_{lsjc}(\hat{r}).$$

The matrix elements are independent of M due to rotational invariance and symmetric under interchange of indices, if the system is time-reversal invariant.

If we group the matrix elements of the coupled equations into matrices,

$$l'\delta_{l'l}\delta_{j'j}\delta_{c'c}\rightarrow L_J \qquad k_{c'}\delta_{l'l}\delta_{j'j}\delta_{c'c}\rightarrow K_J$$
$$\psi^J_{l'j'c',ljc}(r)\rightarrow\Psi_J(r) \qquad \mathsf{U}^J_{l'j'c',ljc}(r)\rightarrow U_J(r)\text{'}$$

we may write the coupled equations for each value of J^π as a matrix equation

$$\left\{\frac{d^2}{dr^2}-\frac{L_J(L_J+1)}{r^2}+K_J^2-\frac{2\mu}{\hbar^2}U_J(r)\right\}\Psi_J(r)=0.$$

The scattering amplitude and S-matrix

We may also introduce the target-spin angular functions into the matrix representation of the partial wave decomposition, but as a vector rather than as a matrix,

$$\mathcal{Y}^{JM}_{lsjc}(\hat{r}) = \langle \hat{r} | lsjcJM \rangle \rightarrow \langle \hat{r} | JM \rangle .$$

The wave function may then be written as

$$\Psi = \frac{4\pi}{r} \sum_{JM} \langle \hat{r} | JM \rangle i^{L_J} \Psi_J(r) e^{i\sigma_J} K_J^{-1} \langle JM | \hat{k} \rangle .$$

Conceptually, obtaining the scattering amplitude is now straightforward. As before, the wave function must be integrated numerically from the origin to beyond the range of the nuclear potential. There, it is matched to either Coulomb or free waves (in matrix form),

$$\Psi_J \rightarrow \frac{i}{2}\left(H_J^-(r) - H_J^+(r) e^{i\sigma_J} \bar{S}_J e^{i\sigma_J} \right) e^{-i\sigma_J} \qquad \text{where} \qquad \bar{S}^J_{l'j'c',ljc} \rightarrow \bar{S}_J .$$

Substituting this expression in the partial wave expansion and analyzing its asymptotic form, we obtain the scattering amplitude,

$$\bar{f}(\theta) = \frac{4\pi}{2i} \sum_{JM} \langle \hat{r} | JM \rangle \left(e^{i\sigma_J} \bar{S}_J e^{i\sigma_J} - 1_J \right) K_J^{-1} \langle JM | \hat{k} \rangle .$$

The matrix elements of the scattering amplitude, $\bar{f}_{\nu' N_c' c', \nu N_c c}$, are labeled by the target state and the projections of the projectile and target spins.

Flux normalization

The cross section can be defined in terms of a ratio of current densities or fluxes. When energy is removed from the relative motion, as in inelastic scattering, the relative velocity and the corresponding flux are reduced. To correct for this, we must multiply the scattering amplitude by a factor of

$$\sqrt{v_f / v_i} = \sqrt{k_f / k_i}.$$

We may do this by defining first the normalized S-matrix,

$$S_J = K_J^{1/2} \bar{S}_J K_J^{-1/2},$$

and then defining the normalized scattering amplitude in its terms as

$$f(\theta) = \frac{4\pi}{2i} \sum_{JM} \left\langle \hat{r} \middle| JM \right\rangle \left(e^{i\sigma_J} S_J e^{i\sigma_J} - 1_J \right) K_J^{-1} \left\langle JM \middle| \hat{k} \right\rangle$$

$$= f_C(\theta) + \frac{4\pi}{2i} \sum_{JM} \left\langle \hat{r} \middle| JM \right\rangle e^{i\sigma_J} \left(S_J - 1_J \right) e^{i\sigma_J} K_J^{-1} \left\langle JM \middle| \hat{k} \right\rangle,$$

where the Coulomb amplitude $f_C(\theta)$ is now a matrix, diagonal in the spin projections and state indices, but different for each of the target states due to the difference in the relative motion..

Angular distributions and cross sections

The angular distributions for an unpolarized beam and target are obtained by averaging the squared amplitude over the initial spin projections and summing over the final ones. Denoting the initial state by c_0 and its spin by I_0, the differential elastic cross section is

$$\frac{d\sigma_{el}}{d\Omega} = \frac{1}{(2s+1)(2I_0+1)} \sum_{\substack{v'N_0' \\ vN_0}} \left| f_{v'N_0'c_0, vN_0c_0}(\theta) \right|^2 .$$

The differential inelastic cross section to an excited state c with spin I_c is

$$\frac{d\sigma_c}{d\Omega} = \frac{1}{(2s+1)(2I_0+1)} \sum_{\substack{v'N_c' \\ vN_0}} \left| f_{v'N_c'c, vN_0c_0}(\theta) \right|^2 .$$

For neutrons, the integrated elastic cross section is

$$\sigma_{el} = \frac{1}{2(2I_0+1)} \frac{\pi}{k_{c_0}^2} \sum_{\substack{l'j' \\ ljJ}} (2J+1) \left| S^J_{l'j'c_0, ljc_0} - \delta_{l'l}\delta_{j'j} \right|^2 .$$

For charged or neutral particles, the inelastic cross section to an excited state c with spin I_c is

$$\sigma_c = \frac{1}{(2s+1)(2I_0+1)} \frac{\pi}{k_{c_0}^2} \sum_{\substack{l'j' \\ ljJ}} (2J+1) \left| S^J_{l'j'c, ljc_0} \right|^2 .$$

Absorption cross sections

Just as in the spherical optical model, we may associate an elastic absorption cross section σ_r with the flux lost from the elastic channel,

$$\sigma_r = -\frac{1}{v}\int_S \vec{j}_{c_0}\cdot d\vec{S} \qquad \text{where} \qquad \vec{j}_{c_0} = \frac{\hbar}{2i\mu}\left(\Psi^{\dagger}_{c_0}\nabla\Psi_{c_0} - \left(\nabla\Psi^{\dagger}_{c_0}\right)\Psi_{c_0}\right),$$

with Ψ_{c_0} being the ground-state component of the wave function. This cross section includes the flux lost to inelastic scattering as well as absorption.

We may also define a total absorption cross section σ_{abs} (which is smaller than the elastic one) as the flux lost from all of the channels together,

$$\sigma_{abs} = -\frac{1}{v}\int_S \sum_c \vec{j}_c\cdot d\vec{S} \qquad \text{where} \qquad \vec{j}_c = \frac{\hbar}{2i\mu}\left(\Psi^{\dagger}_{c}\nabla\Psi_{c} - \left(\nabla\Psi^{\dagger}_{c}\right)\Psi_{c}\right),$$

with Ψ_c the component of the wave function of state c.

We have for the inelastic channels

$$\frac{1}{v}\int_S \vec{j}_c\cdot d\vec{S} = \sigma_c \quad c\neq c_0, \qquad \text{so that} \qquad \sigma_{\mathrm{r}} = \sigma_{abs} + \sum_{c\neq c_0}\sigma_c.$$

That is, the elastic absorption cross section is the sum of the total absorption cross section and the inelastic excitation cross sections.

Cross sections and transmission coefficients

Uing the asymptotic form of the wave function, the elastic absorption cross section may be calculated,

$$\sigma_r = \frac{1}{(2s+1)(2I_0+1)} \frac{\pi}{k_{c_0}^2} \sum_{\substack{l'j' \\ ljJ}} (2J+1)\left(\delta_{l'l}\delta_{j'j} - \left| S^J_{l'j'c_0,ljc_0} \right|^2 \right).$$

It is a sum of the contributions of the elastic S-matrix elements.

The total absorption cross section may be reduced to a similar form,

$$\sigma_{abs} = \frac{1}{(2s+1)(2I_0+1)} \frac{\pi}{k_{c_0}^2} \sum_{ljJ} (2J+1) T^J_{ljc_0,ljc_0},$$

where we have introduced the coupled-channel transmission coefficients, which in matrix form are

$$T_J = 1_J - S_J^\dagger S_J.$$

For neutrons, we may define the total cross section as the sum of the elastic and the elastic absorption ones,

$$\sigma_{tot} = \sigma_{el} + \sigma_r = \frac{1}{(2I_0+1)} \frac{\pi}{k_{c_0}^2} \sum_{ljJ} (2J+1)\left(1 - \mathrm{Re}\, S^J_{ljc_0,ljc_0} \right).$$

The total cross section measures the flux lost from the incident plane wave. It takes into account scattering of any type.

An example – Rotational excitation of ^{238}U

Let us consider excitation of the ground state rotational band of ^{238}U through the 8^+ state. For J=1/2, 1+2+2+2+2=9 coupled channels are involved. For large values of the total angular momentum, we have 1+5+9+13+17=45 coupled channels in each partial wave.

The cross sections of the first excited states increase rapidly above their thresholds. The cross sections of the more highly excited states increase more smoothly.

All of the cross sections decrease very slowly at high energy.

The high energy values of the cross sections decrease by a factor of about 5 for each state as one ascends the rotational band in excitation energy.

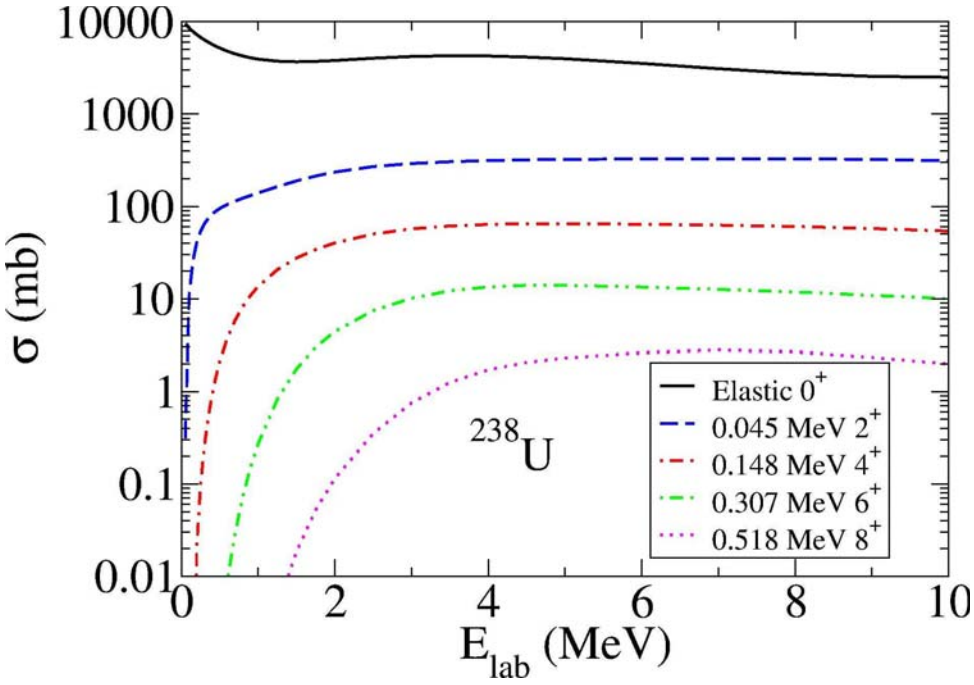

Comparison with experiment

Inelastic cross sections are dominated by the contribution from the compound nucleus at low energies, as seen here for the first excited states of ^{58}Ni and ^{238}U.

The two calculations of the ^{58}Ni inelastic cross section use the same value of β_2=0.2, yet yield cross sections that differ by almost a factor of two due to differences in the optical potentials.

The cross section for excitation of the rotational state in ^{238}U is 5 to 10 times greater than that of the vibrational state in ^{58}Ni, mainly due to the factor of 30 difference in their excitation energies.

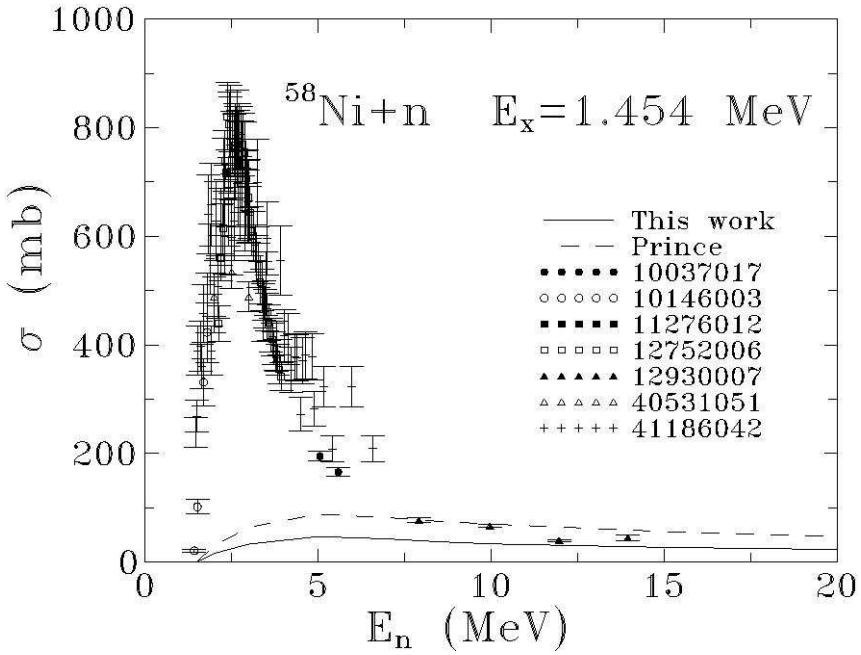

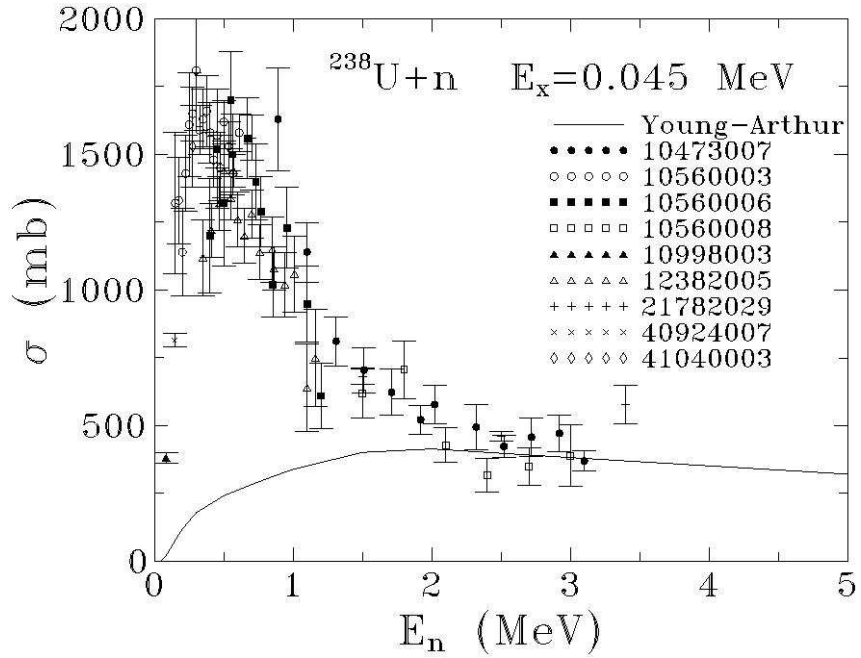

The Lippmann-Schwinger equation -- I

The integral representation of the wave equation, the Lippmann-Schwinger equation,

$$\Psi = \Psi_0 + \left(E^+ - H_0\right)^{-1} U'\Psi = \Psi_0 + G_0^+ U'\Psi, \quad \text{where} \quad (E - H_0)\Psi_0 = 0,$$

is often very useful for the analysis and solution of scattering problems. Here, G_0^+ is the outgoing-wave Green's function and Ψ_0 a wave function with an incoming wave boundary condition. It is usually most convenient to place the single-channel optical potential in the H_0 of the equation and only the couplings between states in U'.

For the single-channel optical model, we can define incoming/outgoing-wave solutions, $h_{lc}^{j\pm}(r)$, of the wave equation,

$$\left(\frac{d^2}{dr^2} - \frac{l(l+1)}{r^2} + k_c^2 - \frac{2\mu}{\hbar^2}\left(U_{cen,c}(r) + d_l^j U_{so,c}(r)\right) \right) h_{lc}^{j\pm}(r) = 0,$$

where the spin-orbit factor is $d_l^j = d_{so}\left(j(j+1) - l(l+1) - s(s+1)\right)/2.$

Asymptotically, these solutions behave as incoming/outgoing Coulomb (free) waves,

$$h_{lc}^{j\pm}(r) \to H_{lc}^{j\pm}(r) = e^{\mp i\sigma_{lc}}\left(G_{lc}(r) \pm iF_{lc}(r)\right).$$

The Lippmann-Schwinger equation -- II

The solution to the single-channel Schrödinger equation that is regular at the origin is given in terms of the incoming/outgoing solutions and the S-matrix as

$$\psi_{lc}^{j+}(r) = \frac{i}{2}\left(h_{lc}^{j-}(r) - h_{lc}^{j+}(r) e^{2i\sigma_{lc}} S_{0lc}^{j} \right) = \psi_{lc}^{j}(r) e^{i\sigma_{lc}} ,$$

which is just the single-channel wave function of the partial wave expanson. We have merely relabeled the S-matrix as S_0.

The single-channel Green's function may be decomposed in partial waves as

$$G_{0c}^{+}(\vec{r},\vec{r}\,') = \frac{1}{rr'} \sum_{ljn} \mathrm{Y}_{ls}^{jn}(\hat{r}) g_{lc}^{j+}(r,r') \mathrm{Y}_{ls}^{jn\dagger}(\hat{r}'),$$

where

$$g_{lc}^{j+}(r,r') = -\frac{2\mu}{\hbar^2 k_c} \psi_{lc}^{j}(r_<) e^{i\sigma_{lc}} h_{lc}^{j+}(r_>).$$

The complete single-channel Green's function for the coupled-channels problem may then composed as

$$G_0^{+}(\vec{r},\vec{r}\,') = \sum_{cN_c} \left| cI_c N_c \right\rangle G_{0c}^{+}(\vec{r},\vec{r}\,') \left\langle cI_c N_c \right|$$

$$= \frac{1}{rr'} \sum_{ljn} \mathrm{Y}_{lsj}^{JM}(\hat{r}) g_{lc}^{j+}(r,r') \mathrm{Y}_{lsj}^{JM\dagger}(\hat{r}').$$

The Lippmann-Schwinger equation -- III

In terms of the channel matrices, the Green's function G_0^+ takes the form

$$G_0^+(\vec{r},\vec{r}\,') = \frac{1}{rr'}\sum_{JM}\left\langle \hat{r}\middle| JM\right\rangle G_{0J}^+(r,r')\left\langle JM\middle|\hat{r}\,'\right\rangle,$$

where we have grouped the appropriate Green's functions in diagonal matrices,

$$g_{lc}^{j+}(r,r')\delta_{l'l}\delta_{j'j}\delta_{c'c} \to G_{0J}^+(r,r').$$

In terms of these, we can write the contribution to the Lippmann-Schwinger equation of each partial wave as

$$\Psi_J(r) = \Psi_{0J}(r) + \int_0^\infty dr'\, G_{0J}^+(r,r')U_J'(r')\Psi_J(r').$$

Substituting the large-r expressions for the wave functions,

$$\Psi_{\substack{J,\\ 0J}} \to \frac{i}{2}\left(H_J^-(r) - H_J^+(r)e^{i\sigma_J}\bar{S}_{\substack{J,\\ 0J}}e^{i\sigma_J}\right)e^{-i\sigma_J},$$

and using flux conservation to normalize the S-matrix, $S_J = K_J^{1/2}\bar{S}_J K_J^{-1/2}$, we obtain

$$S_J = S_{0J} + 2i\frac{2\mu}{\hbar^2}K_J^{-1/2}\int_0^\infty dr'\,\Psi_{0J}(r')U_J'(r')\Psi_J(r')K_J^{-1/2}.$$

The distorted-wave Born approximation (DWBA)

The Lippmann-Schwinger equation,

$$\Psi_J(r) = \Psi_{0J}(r) + \int_0^\infty dr'\, G^+_{0J}(r,r')U'_J(r')\Psi_J(r'),$$

here in partial wave form, contains the wave function $\Psi_J(r)$ on both the right and left sides of the equation. This can be used to advantage when the coupling potential U' is small. We then expect the wave function Ψ_J to be little different from the uncoupled one Ψ_{0J}, so that we have, to first order,

$$\Psi^{(1)}_J(r) = \Psi_{0J}(r) + \int_0^\infty dr'\, G^+_{0J}(r,r')U'_J(r')\Psi_{0J}(r').$$

The corresponding DWBA S-matrix is

$$S^{(1)}_J = S_{0J} + 2i\frac{2\mu}{\hbar^2}K_J^{-1/2}\int_0^\infty dr'\,\Psi_{0J}(r')U'_J(r')\Psi_{0J}(r')K_J^{-1/2}.$$

The DWBA approximation may be extended to higher orders by substituting the solution of the previous order in the Lippmann-Schwinger equation. The second-order solution, for example, is obtained by substituting the first order solution in the integral equation. However, the DWBA is usually not used above the second-order.

Limit of the DWBA

Two examples give us an idea of when the DWBA might be applied to inelastic scattering.

The DWBA provides a reasonable approximation to excitation of a vibrational state such as the 2^+ one in ^{58}Ni. However, it greatly overestimates the excitation of a strongly-excited rotational state, such as the 2^+ one in ^{238}U.

In general, the DWBA overestimates the inelastic cross section, since it does not take into account transitions back to the ground state.

In the case of ^{238}U, we note that transitions to other states of the rotational band can also be important.

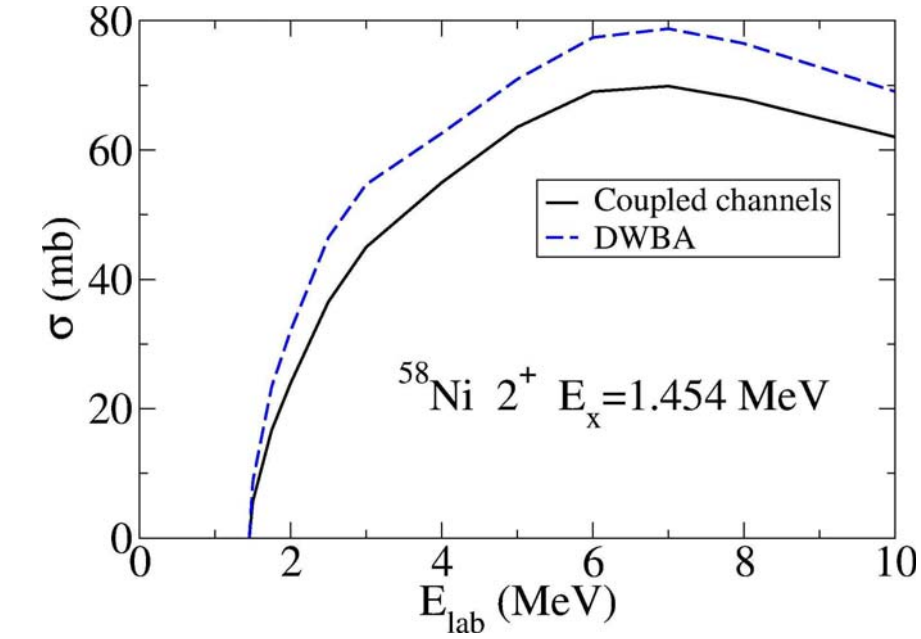

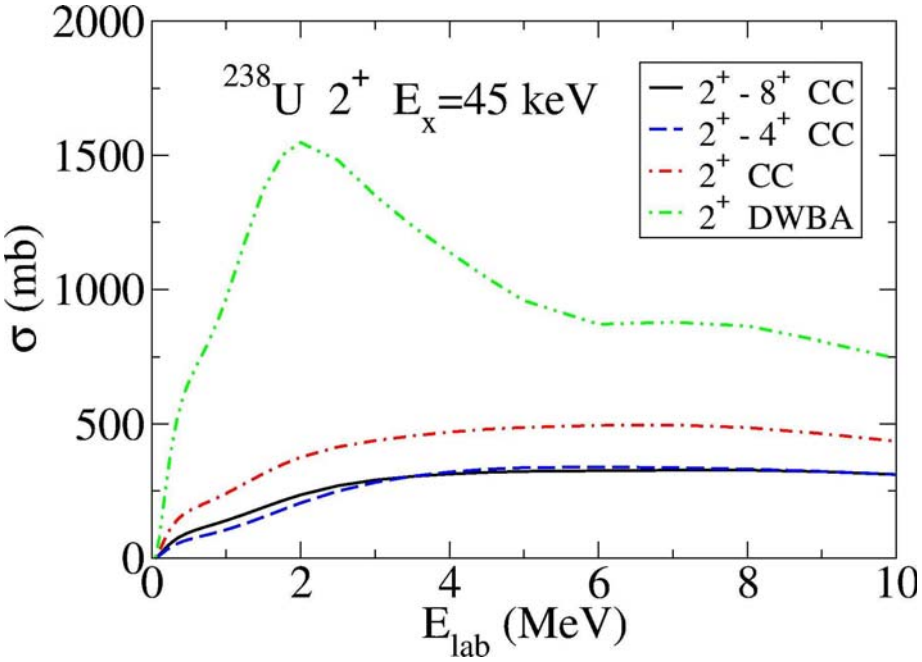

Multistep direct reactions

The multistep direct model is a direct extension of the DWBA treatment of weakly excited levels that takes into account the possibility of multiple interactions. The differential cross section is written as an incoherent sum of one-step and multistep terms,

$$\frac{d^2\sigma_{b\leftarrow a}(E,\Omega\leftarrow E_0,\Omega_0)}{dEd\Omega}=\sum_{n=1}^{\infty}\frac{d^2\sigma^{(n)}_{b\leftarrow a}(E,\Omega\leftarrow E_0,\Omega_0)}{dEd\Omega}.$$

The one-step cross section is calculated by summing the DWBA cross sections to the particle-hole states μ, weighted by a broadened density of states $\hat{\rho}_{11}$,

$$\frac{d^2\sigma^{(1)}_{b\leftarrow a}(E,\Omega\leftarrow E_0,\Omega_0)}{dEd\Omega}=\sum_{\mu}\hat{\rho}_{11}(E_0-E,\mu)\frac{d^2\sigma^{DWBA}_{b\leftarrow a,\mu}(E,\Omega\leftarrow E_0,\Omega_0)}{d\Omega}.$$

The n-step cross section is then usually calculated by convoluting the (n-1)-step cross section and summing over all intermediate configurations,

$$\frac{d^2\sigma^{(n)}_{b\leftarrow a}(E,\Omega\leftarrow E_0,\Omega_0)}{dEd\Omega}=\frac{m}{(2\pi\hbar)^2}\sum_c\int E'dE'd\Omega'\frac{d^2\sigma^{(1)}_{b\leftarrow c}(E,\Omega\leftarrow E',\Omega')}{dEd\Omega}$$

$$\times\frac{d^2\sigma^{(n'-1)}_{c\leftarrow a}(E',\Omega'\leftarrow E_0,\Omega_0)}{dE'd\Omega'}.$$

Summary

The objective of the optical model is to describe the fast, direct contribution to nuclear scattering. It makes use of an optical potential having both real and negative imaginary parts. The absorption of flux from the optical wave function, due to the imaginary part of the potential, accounts for the flux lost to the slower, compound nucleus component of the scattering.

The single-channel optical model describes the scattering in the elastic channel alone. It is often called the spherical optical model because, in it, the target may be considered to be spherically symmetric, since its structure is never introduced.

Direct reactions that transfer energy as well as momentum are often quite important. Such inelastic scatterings, in the case of the inert projectiles that we are considering (n, p, α, d, etc.), leave the target in an excited state and diminish the asymptotic kinetic energy of the projectile. To describe inelastic scattering, one must introduce at least the basic characteristics of the ground and excites states of the target.